Effect of an Inducer of BiP, a Molecular Chaperone, on Endoplasmic Reticulum (ER) Stress-Induced Retinal Cell Death

Yuta Inokuchi,[1] *Yoshimi Nakajima,*[1] *Masamitsu Shimazawa,*[1] *Takanori Kurita,*[2] *Mikiko Kubo,*[3] *Atsushi Saito,*[4] *Hironao Sajiki,*[2] *Takashi Kudo,*[3] *Makoto Aihara,*[5] *Kazunori Imaizumi,*[4] *Makoto Araie,*[5] *and Hideaki Hara*[1]

Purpose. The effect of a preferential inducer of 78 kDa glucose-regulated protein (GRP78)/immunoglobulin heavy-chain binding protein (BiP; BiP inducer X, BIX) against tunicamycin-induced cell death in RGC-5 (a rat ganglion cell line), and also against tunicamycin- or *N*-methyl-D-aspartate (NMDA)-induced retinal damage in mice was evaluated.

Methods. In vitro, BiP mRNA was measured after BIX treatment using semi-quantitative RT-PCR or real-time PCR. The effect of BIX on tunicamycin (at 2 μg/mL)-induced damage was evaluated by measuring the cell-death rate and CHOP protein expression. In vivo, BiP protein induction was examined by immunostaining. The retinal cell damage induced by tunicamycin (1 μg) or NMDA (40 nmol) was assessed by examining ganglion cell layer (GCL) cell loss, terminal deoxyribonucleotidyl transferase (TdT)-mediated dUTP nick-end labeling (TUNEL) staining, and CHOP protein expression.

Results. In vitro, BIX preferentially induced BiP mRNA expression both time- and concentration-dependently in RGC-5 cells. BIX (1 and 5 μM) significantly reduced tunicamycin-induced cell death, and BIX (5 μM) significantly reduced tunicamycin-induced CHOP protein expression. In vivo, intravitreal injection of BIX (5 nmol) significantly induced BiP protein expression in the mouse retina. Co-administration of BIX (5 nmol) significantly reduced both the retinal cell death and the CHOP protein expression in GCL induced by intravitreal injection of tunicamycin or NMDA.

Conclusions. These findings suggest that this BiP inducer may have the potential to be a therapeutic agent for endoplasmic reticulum (ER) stress-induced retinal diseases. (*Invest Ophthalmol Vis Sci.* 2009;50:334-344) DOI:10.1167/iovs.08-2123

The endoplasmic reticulum (ER) is the cellular organelle in which proteins (destined for secretion or for diverse subcellular localizations) are not only synthesized, but acquire their correct conformation. Perturbations of the environment normally required for protein folding in the ER, or the production of large amounts of misfolded proteins exceeding the functional capacity of the organelle, trigger a pattern of physiological response in the cell, collectively known as the unfolded protein response (UPR).[1-3] The UPR serves to cope with ER stress by transcriptionally regulating ER chaperones and other ER-resident proteins, attenuating the overall translation rate, and increasing the degradation of misfolded ER proteins. ER stress is caused by the accumulation of unfolded proteins in the ER lumen, and it is associated with various neurodegenerative diseases such as Alzheimer's, Huntington's, and Parkinson's diseases, and with type-1 diabetes.[4-6] Recent reports have shown that ER stress is also involved in a variety of experimental retinal neurodegenerative models, such as those of diabetic retinopathy,[7] retinitis pigmentosa,[8,9] and glaucoma.[10,11]

Recently, we reported that BiP expression is upregulated in the retina after intravitreal injection of either tunicamycin or NMDA (a glutamate-receptor agonist).[12,13] Tunicamycin, a glucosamine-containing nucleoside antibiotic, produced by genus *Streptomyces*, is an inhibitor of *N*-linked glycosylation and the formation of *N*-glycosidic protein-carbohydrate linkages.[14] Tunicamycin, which reduces the *N*-glycosylation of proteins, causes an accumulation of unfolded proteins in the ER and thus induces ER stress. Awai et al.[15] previously had demonstrated that NMDA induces CHOP protein (a member of the CCAAT/enhancer-binding protein family induced by ER stress) in GCL and the inner plexiform layer (IPL), and that CHOP$^{-/-}$ mice are more resistant to NMDA-induced retinal cell death than wild-type mice. These findings indicate that ER stress may be involved in these models of retinal injury.

BiP, a highly conserved member of the 70 kDa heat shock protein family, is one of the chaperones localized to the ER membrane,[16,17] and it is a major ER-luminal Ca^{2+}-storage protein.[18,19] BiP works to restore folding in misfolded or incompletely assembled proteins,[20-22] the interaction between BiP and misfolded proteins being dependent on its hydrophobic motifs.[23-25] Proteins stably bound to BiP are subsequently translocated from the ER into the cytosol, where they are degraded by proteasomes.[26,27] Previous reports have show that induction of BiP prevents the neuronal death induced by ER stress.[28-31] Hence, a selective inducer of BiP might attenuate ER stress and be a new, useful therapeutic agent for the treatment of ER stress-associated diseases.

This seemed an interesting idea, and we recently identified BiP inducer X (BIX) while screening for low molecular

From the Departments of [1]Biofunctional Evaluation, Molecular Pharmacology and [2]Medicinal Chemistry, Gifu Pharmaceutical University, Gifu, Japan; [3]Department of Psychiatry, Osaka University Graduate School of Medicine, Osaka, Japan; [4]Division of Molecular and Cellular Biology, Department of Anatomy, Faculty of Medicine, University of Miyazaki, Miyazaki, Japan; and [5]Department of Ophthalmology, University of Tokyo School of Medicine, Tokyo, Japan.

Supported in part by a Grant-in-Aid (No.18209053) for scientific research from the Ministry of Education, Science, Sports, Culture of the Japanese Government; by a research grant (No.18210101) from the Ministry of Health, Labor, and Welfare of the Japanese Government, and by Grant-in-Aid for Japan Society for the Promotion of Science Fellows.

Submitted for publication April 4, 2008; revised July 25, 2008; accepted October 27, 2008.

Disclosure: **Y. Inokuchi**, None; **Y. Nakajima**, None; **M. Shimazawa**, None; **T. Kurita**, None; **M. Kubo**, None; **A. Saito**, None; **H. Sajiki**, None; **T. Kudo**, None; **M. Aihara**, None; **K. Imaizumi**, None; **M. Araie**, None; **H. Hara**, None

The publication costs of this article were defrayed in part by page charge payment. This article must therefore be marked "*advertisement*" in accordance with 18 U.S.C. §1734 solely to indicate this fact.

Corresponding author: Hideaki Hara, Department of Biofunctional Evaluation, Molecular Pharmacology, Gifu Pharmaceutical University, 5-6-1 Mitahora-higashi, Gifu 502-8585, Japan; hidehara@gifu-pu.ac.jp.

Investigative Ophthalmology & Visual Science, January 2009, Vol. 50, No. 1

mass compounds that might induce BiP using high-throughput screening (HTS) with a BiP reporter assay system (Dual-Luciferase Reporter Assay; Promega Corporation, Madison, WI).[32] We found that BIX preferentially induced BiP mRNA and protein in SK-N-SH cells and reduced tunicamycin-induced cell death. Intracerebroventricular pretreatment with BIX reduced the infarction size after focal cerebral ischemia in mice. In view of the retinal research described above, we wondered whether BIX might reduce the retinal ganglion cell loss and CHOP expression induced by tunicamycin or NMDA treatment.

In the present study, we examined primarily whether induction of BiP might inhibit the retinal cell death induced by tunicamycin in RGC-5 cells in vitro, and/or that induced by tunicamycin or NMDA in mice in vivo.

Materials and Methods

All experiments were performed in accordance with the ARVO Statement for the Use of Animals in Ophthalmic and Vision Research, and they were approved and monitored by the Institutional Animal Care and Use Committee of Gifu Pharmaceutical University, Gifu, Japan.

Materials

Dulbecco modified Eagle medium (DMEM) and NMDA were purchased from Sigma-Aldrich (St. Louis, MO). The other drugs used and their sources were as follows: BIX, 1-(3,4-dihydroxyphenyl)-2-thiocyanatoethanone, was synthesized in the Department of Medicinal Chemistry, Gifu Pharmaceutical University, while tunicamycin was purchased from Wako (Osaka, Japan). Isoflurane was acquired from Nissan Kagaku (Tokyo, Japan) and fetal bovine serum (FBS) was from Valeant (Costa Mesa, CA).

RGC-5 Culture

RGC-5[32] were gifted by Neeraj Agarwal (Department of Pathology and Anatomy, UNT Health Science Center, Fort Worth, TX). Cultures of RGC-5 were maintained in DMEM supplemented with 10% FBS, 100 U/mL penicillin (Meiji Seika Kaisha Ltd., Tokyo, Japan), and 100 μg/mL streptomycin (Meiji Seika Kaisha. Ltd.) in a humidified atmosphere of 95% air and 5% CO_2 at 37°C. The RGC-5 cells were passaged by trypsinization every 3 days, as in our previous reports.[12,13,33] We used RGC-5 without any differentiation.

RNA Isolation and Semi-Quantitative RT-PCR Analysis

To examine the effect of BIX on BiP mRNA expression, RGC-5 cells were seeded in six-well plates at a density of 1.4×10^5 cells per well. After the cells had been incubating for 24 h, they were exposed to 50 μM BIX in 1% FBS DMEM for 0.5, 1, 2, 4, 6, 8, or 12 h, or to 2, 10, 50, or 150 μM BIX in 1% FBS DMEM for 6 h. Total RNA was extracted (RNeasy Mini Kit; QIAGEN KK, Tokyo, Japan) according to the manufacture's protocol. The total RNA was divided into microtubes, and frozen to −80°C. RNA concentrations were determined spectrophotometrically at 260 nm. First-strand cDNA was synthesized in a 20-μl reaction volume using a random primer (Takara, Shiga, Japan) and Moloney murine leukemia virus reverse transcriptase (Invitrogen, Carlsbad, CA). PCR was performed in a total volume of 30 μL containing 0.8 μM of each primer, 0.2 mM dNTPs, 3 U *Taq* DNA polymerase (Promega), 2.5 mM $MgCl_2$, and 1× PCR buffer. The amplification conditions for the semi-quantitative RT-PCR analysis were as follows: an initial denaturation step (95°C for 5 minutes), 20 cycles of 95°C for 1 minute, 55°C for 1 minute, and 72°C for 1 minute, and a final extension step (72°C for 7 minutes). The numbers of amplification cycles for the detection of BiP and β-actin were 18 and 15, respectively. The primers used for amplification were as follows: BiP: 5′-GTTTGCTGAGGAAGACAAAAAGCTC-3′ and 5′-CACTTCCATAGAGTTTGCTGATAATTG-3′; β-actin: 5′-TCCTCCCTGGAGAAGAGCTAC-3′ and 5′-TCCTGCTTGCTGATCCACAT-3′.

PCR products were resolved by electrophoresis through 6% (w/v) polyacrylamide gels. The density of each band was quantified using an imaging program (Scion Image Program; Scion Corporation, Frederick, MD).

Real-Time PCR

Real-time PCR (TaqMan; Applied Biosystems, Foster City, CA) was performed as described previously.[34] Single-stranded cDNA was synthesized from total RNA using a high-capacity cDNA archive kit (Applied Biosystems). Quantitative real-time PCR was performed using a sequence detection system (ABI PRISM 7900HT; Applied Biosystems) with a PCR master mix (TaqMan Universal PCR Master Mix; Applied Biosystems), according to the manufacturer's protocol. mRNA expression was measured by real-time PCR using a gene expression product (Assays-on-Demand Gene Expression Product; Applied Biosystems) and a BiP probe (Assay ID Details: Mm00517691). The thermal cycler conditions were as follows: 2 minutes at 50°C and then 10 minutes at 95°C, followed by two-step PCR for 50 cycles consisting of 95°C for 15 seconds followed by 60°C for 1 minute. For each PCR, we obtained the slope value, R^2 value, and linear range of a standard curve of serial dilutions. All reactions were performed in duplicate. The results are expressed relative to the β-actin (Assay ID Details: Mm00661904) internal control.

Cell Viability

To examine the effects of BIX on the cell death induced by tunicamycin (2 μg/mL) or staurosporine (an ER stress-independent apoptosis inducer, 30 nm) RGC-5 cells were seeded at a low density of 700 cells per well into 96-well plates. After pretreatment with BIX for 12 h, tunicamycin or staurosporine was added to the cultures for 48 h or 24 h, respectively. Cell death was assessed on the basis of combination staining with the fluorescent dyes Hoechst 33342 and propidium iodide (PI; Molecular Probes, Eugene, OR) or the change in fluorescence intensity after the cellular reduction of WST-8 to formazan. Hoechst 33342 (λex 350 nm, λem 461 nm) and PI (λex 535 nm, λem 617 nm) were added to the culture medium at final concentrations of 8 and 1.5 μM, respectively, for 30 minutes. Images were collected using a CCD camera (DP30VW; Olympus America, Center Valley, PA) via an epifluorescence microscope (IX70; Olympus, Tokyo, Japan) fitted with fluorescence filters for Hoechst 33342 (U-MWU; Olympus), and PI (U-MWIG; Olympus). In WST-8 assay, cell viability was assessed by culturing cells in a culture medium containing 10% WST-8 (Cell Counting Kit-8; Dojin Kagaku, Kumamoto, Japan) for 3 h at 37°C, with quantification being achieved by scanning with a microplate reader at 492 nm.[35] This absorbance is expressed as a percentage of that in control cells (which were in 1% FBS DMEM) after subtraction of background absorbance.

Animals

Mice used were male adult ddY mice (Japan SLC, Hamamatsu, Japan), male adult Thy-1-cyan fluorescent protein (CFP) transgenic mice (The Jackson Laboratory, Bar Harbor, Maine),[36] and ER stress-activated indicator (ERAI)-transgenic mice carrying the F-XBP1ΔDBD-venus, a variant of green fluorescent protein (GFP) fusion gene, which allows effective identification of cells under ER stress in vivo, as previously described by Iwawaki et al.[37] Briefly, when ER stress in ERAI transgenic mice was induced, splicing of mRNA encoding the XBP-1 fusion gene occurs and the spliced form of F-XBP1ΔDBD-venus fusion gene could be translated into fluorescent protein. Thus, it is visualized by the fluorescence intensity arising from the XBP-Δ-venus fusion protein during ER stress, and we measured it by fluorescence microscopy and immunoblotting in the present study.

All mice were kept under controlled lighting conditions (12 h:12 h light/dark). The mouse genotype was determined by applying standard PCR methodology to tail DNA.

NMDA- or Tunicamycin-Induced Retinal Damage

NMDA- or tunicamycin-induced retinal damage was produced as previously reported by Siliprandi et al. (1992).[38] Briefly, mice were anesthetized with 3.0% isoflurane and maintained with 1.5% isoflurane in 70% N_2O and 30% O_2 via an animal general anesthesia machine (Soft Lander; Sin-ei Industry Co. Ltd., Saitama, Japan). The body temperature was maintained between 37.0 and 37.5°C with the aid of a heating pad. Retinal damage was induced by the injection (2 μL/eye) of NMDA (Sigma-Aldrich) at 20 mM or tunicamycin at 1 μg/mL dissolved in 0.01 M PBS with 5% dimethyl sulfoxide (DMSO). Each solution was injected into the vitreous body of the left eye under the above anesthesia. One drop of 0.01% levofloxacin ophthalmic solution (Santen Pharmaceuticals Co. Ltd., Osaka, Japan) was applied topically to the treated eye immediately after the intravitreal injection. Seven days after the injection, eyeballs were enucleated for histologic analysis. For comparative purposes, nontreated retinas from each mouse strain were also investigated. BIX (0.5 or 5 nmol) or vehicle (5% DMSO in PBS) was co-administered with the NMDA or tunicamycin in each mouse.

Histologic Analysis

In mice under anesthesia produced by an intraperitoneal injection of sodium pentobarbital (80 mg/kg), each eye was enucleated and kept immersed for at least 24 h at 4°C in a fixative solution containing 4% paraformaldehyde. Six paraffin-embedded sections (thickness, 4 μm) cut through the optic disc of each eye were prepared in a standard manner and stained with hematoxylin and eosin. The damage induced by NMDA or tunicamycin was then evaluated, with three sections from each eye being used for the morphometric analysis, as described below. Light-microscope images were photographed, and the cells in the GCL at a distance between 375 and 625 μm from the optic disc were counted on the photographs in a masked fashion by a single observer (Y.I.). Data from three sections (selected randomly from the six sections) were averaged for each eye and used to evaluate the cell count in the GCL.

Retinal Flatmounts and Analysis in Transgenic Mice

Transgenic mice were given an overdose of sodium pentobarbital, and retinas were dissected out and fixed for 30 minutes in 4% paraformaldehyde diluted in 0.1 M phosphate buffer (PB) at pH 7.4. Retinas were subsequently washed with PBS at room temperature, flatmounted on clean glass slides using fluorescent mounting medium (Dako Corp., Carpinteria, CA), and stored in the dark at 4°C for 1 week. The damage induced by tunicamycin was then evaluated, with four sections (dorsal, ventral, temporal, and nasal) from each eye being used for the morphometric analysis, as described below. At various times after intravitreal injections (24 h in ERAI mice and 7 days in Thy-1-CFP transgenic mice), fluorescent images were photographed (×200, 0.144 mm^2) using an epifluorescence microscope (BX50; Olympus) fitted with a CCD camera (DP30VW; Olympus). In the case of Thy-1-CFP transgenic mice, Thy-1-CFP-positive cells at a distance of 1 mm from the optic disc were counted on the photographs in a masked fashion by a single observer (Y.I.). Data from the four parts of each eye were used to evaluate the RGC count.[39]

Immunostaining

Eyes were enucleated as described under Histologic Analysis, fixed in 4% paraformaldehyde overnight at 4°C, immersed in 25% sucrose for 48 h at 4°C, and embedded in optimum cutting temperature (OCT) compound (Sakura Finetechnical Co. Ltd, Tokyo, Japan). Transverse 10-μm thick cryostat sections were cut and placed onto slides (MAS COAT; Matsunami Glass Ind., Ltd., Osaka, Japan). Immunohistochemical staining was performed according to the following protocol: Briefly, tissue sections were washed in 0.01 M PBS for 10 minutes, and then endogenous peroxidase was quenched by treating the sections with 3% hydrogen peroxide in absolute methanol for 10 minutes, followed by a pre-incubation with 10% normal goat serum. They were then incubated overnight at 4°C with the following primary antibodies: against CHOP (1:1000 dilution in PBS; Santa Cruz, CA), and against BiP/GRP78 (1:1000 dilution in PBS; BD Transduction Laboratories, Lexington, KY). Sections were washed and then incubated with biotinylated anti-rabbit IgG or anti-mouse IgG. They were subsequently incubated with the avidin-biotin-peroxidase complex for 30 minutes, and then developed using diaminobenzidine (DAB) peroxidase substrate. Images were obtained using a digital camera (COOLPIX 4500; Nikon, Tokyo, Japan).

Quantitation of Density

In the DAB-labeled areas of anti-BiP/GRP78 (BD Transduction Laboratories) and anti-CHOP (Santa Cruz) in the GCL and IPL at a distance between 475 and 525 μm (50 × 50 μm) from the optic disc, retinal DAB-labeled cell density was evaluated by means of appropriately calibrated computerized image analysis, using median density in the range of 0 to 255 as an analysis tool (Image Processing and Analysis in Java, Image J; National Institute of Mental Health, Bethesda, MD) and averaged for two areas.[40] The data lie within the dynamic range of this assays

Briefly, light-microscope images of the above-mentioned areas were photographed, inverted in a gradation sequence using image editing software (Adobe Photoshop 5.5; Adobe Systems Inc., San Jose, CA), and then optical intensity was evaluated using Image J. The score for the negative-control (nontreated with first antibody), as the background value, was subtracted from the scores.

TUNEL Staining

TUNEL staining was performed according to the manufacturer's protocol (In Situ Cell Death Detection Kit; Roche Biochemicals, Mannheim, Germany) to detect the retinal cell death induced by NMDA. Mice were anesthetized with pentobarbital sodium at 80 mg/kg, IP, 24 h after intravitreal injection (either of NMDA 40 nmol/eye or of tunicamycin 1 μg/eye). The eyes were enucleated, fixed overnight in 4% paraformaldehyde, and immersed for 2 days in 25% sucrose with PBS. The eyes were then embedded in a supporting medium (OCT compound) for frozen-tissue specimens. Retinal sections at 10-μm thick were cut on a cryostat at −25°C, and stored at −80°C until staining. After twice washing with PBS, sections were incubated with terminal TdT enzyme at 37°C for 1 h, then washed 3 times in PBS for 1 minute at room temperature. Sections were subsequently incubated with an anti-fluorescein antibody-peroxidase conjugate at room temperature in a humidified chamber for 30 minutes, then developed using DAB tetrahydrochloride peroxidase substrate. Light-microscope images were photographed, and the labeled cells in the GCL at a distance between 375 and 625 μm from the optic disc were counted in two areas of the retina in a masked fashion by a single observer (Y.I.). The number of TUNEL-positive cells was averaged for these two areas, and plotted as the number of TUNEL-positive cells.

Western Blot Analysis

RGC-5 cells were lysed using a cell-lysis buffer (RIPA buffer R0278; Sigma-Aldrich) with protease (P8340; Sigma-Aldrich) and phosphatase inhibitor cocktails (P2850 and P5726; Sigma-Aldrich), and 1 mM EDTA. In vivo, mice were euthanatized using sodium pentobarbital at 80 mg/kg, IP, and their eyeballs were quickly removed. The retinas were carefully separated from the eyeballs and quickly frozen in dry ice. For protein extraction, the tissue was homogenized in the cell-lysis buffer using a homogenizer (Physcotron; Microtec Co. Ltd., Chiba, Japan). The lysate was centrifuged at 12,000*g* for 20 minutes, and the supernatant was used for this study. Assays to determine the protein concentration were performed by comparison with a known concentration of bovine serum albumin using a BCA protein assay kit (Pierce Biotechnology, Rockford, IL). A mixture of equal parts of an aliquot of

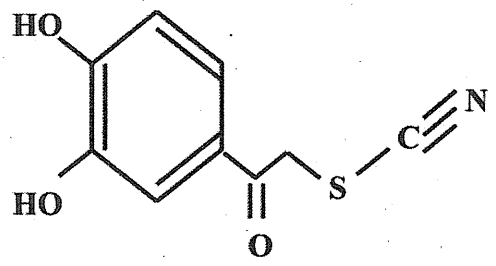

FIGURE 1. The structure of BIX (1-(3,4-dihydroxyphenyl)-2-thiocyanate-ethanone).

protein and sample buffer with 10% 2-mercaptoethanol was subjected to 10% sodium dodecyl sulfate-polyacrylamide gel electrophoresis. The separated protein was then transferred onto a polyvinylidene difluoride membrane (Immobilon-P; Millipore Corporation, Bedford, MA). For immunoblotting, the following primary antibodies were used: rabbit anti-CHOP polyclonal antibody (1:1000; Santa Cruz), mouse anti-β-actin monoclonal antibody (1:4000; Sigma-Aldrich), and rabbit anti-green fluorescent protein (GFP) polyclonal antibody (1:1000; Medical & Biological Laboratories Co. Ltd., Nagoya, Japan). The secondary antibody used was either goat anti-rabbit HRP-conjugated (1:2000) or goat anti-mouse HRP-conjugated (1:2000). The immunoreactive bands were visualized using a chemiluminescent substrate (SuperSignal West Femto Maximum Sensitivity Substrate; Pierce Biotechnology). The band intensity was measured using an imaging analyzer (Lumino Imaging Analyzer; Toyobo, Osaka, Japan) and a gel analysis electrophoresis analysis software (Gel Pro Analyzer; Media Cybernetics, Atlanta, GA).

Statistical Analysis

Data are presented as the means ± SE. Statistical comparisons were made by way of Dunnett's test or Student's *t*-test using statistical analysis software (STAT VIEW version 5.0; SAS Institute, Cary, NC). $P < 0.05$ was considered to indicate statistical significance.

RESULTS

BiP mRNA in RGC-5 Preferentially Induced by BIX

To clarify whether BIX (Fig. 1) induces BiP in RGC-5, we used semi-quantitative RT-PCR and real-time PCR, using a specific primer and a TaqMan probe recognizing BiP mRNA, respectively. Real-time PCR revealed that the level of BiP mRNA was significantly elevated at 0.5 to 12 h (peak at approximately 6 h) after treatment with 50 μM BIX (Fig. 2A). At 6 h after treatment with BIX (2 to 150 μM), BiP mRNA was increased concentration-dependently (Fig. 2B). Next, we used real-time *PCR* to investigate whether BIX might affect the expressions of any other genes related to the ER stress response, such as GRP94, calreticulin, protein kinase inhibitor of 58 kDa ($p58^{IPK}$), or asparagine synthetase (ASNS; Fig. 2C). Real-time PCR revealed significant inductions of ASNS and calreticulin mRNAs at 6 h after treatment with BIX at 2 and 10 μM, respectively. At 50 μM, BIX induced the mRNAs for GRP94 at 12 h, calreticulin at 6 and 12 h, $p58^{IPK}$ at 6 h, and ASNS at 12 h. In contrast, GRP94 mRNA was significantly reduced at 4 h after treatment with 50 μM BIX.

Protective Effect of BIX against ER Stress–Induced Cell Death in RGC-5 Cells

To investigate whether BIX can prevent the cell death induced by ER stress, RGC-5 cells were pretreated for 12 h with or without BIX, then treated with 2 μg/mL tunicamycin, and finally incubated for a further 48 h. Fluorescence micrographs of Hoechst 33342 and PI staining revealed 38.4 ± 4.5% cell death ($n = 8$) at 48 h after tunicamycin treatment, (control: 0.9 ± 0.2%, $n = 8$), and pretreatment with BIX at 1 and 5 μM significantly reduced this cell death (Figs. 3A, 3B). Next, we evaluated the expression of CHOP protein after tunicamycin treatment. There was no CHOP protein expression in either nontreated or BIX-treated cells (Figs. 3C, 3D). On the other

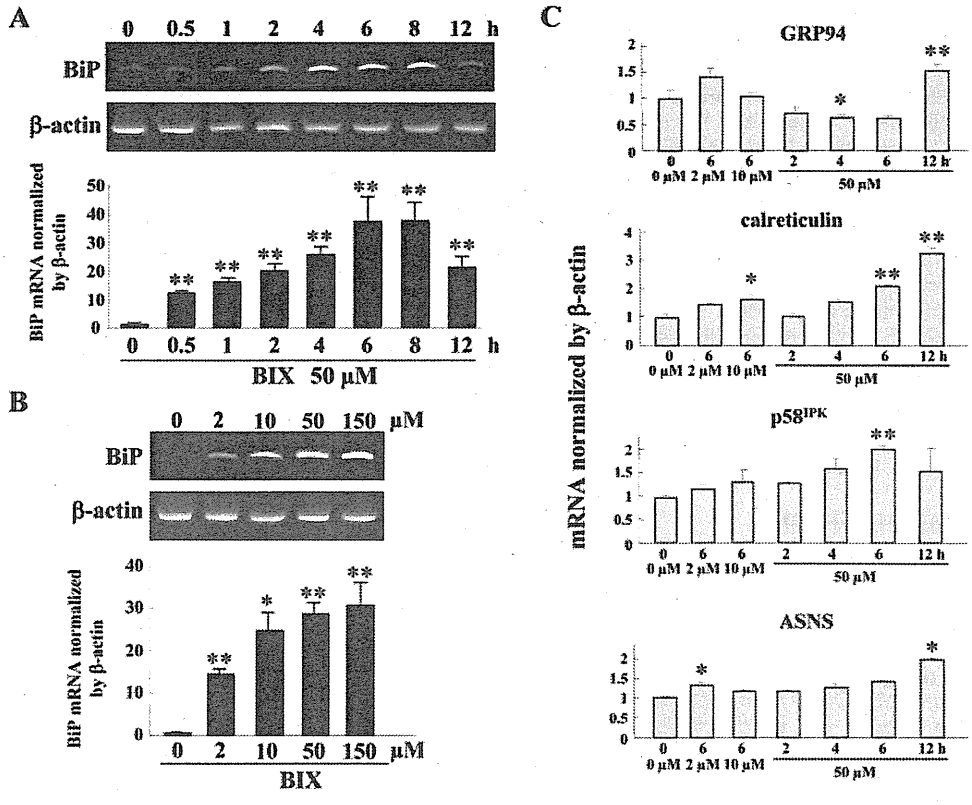

FIGURE 2. Effect of BIX on BiP mRNA expression BIX in RGC-5 cells. (**A**) Time-dependent induction of BiP mRNA after treatment with 50 μM BIX and (**B**) concentration-dependence of BIX-induced BiP mRNA expression are each shown by semi-quantitative RT-PCR (*upper panel*) and real-time PCR (*lower panel*). β-Actin mRNA is shown as an internal control. (**C**) Induction of GRP94, calreticulin, $p58^{IPK}$, and ASNS mRNAs at 6 h after treatment with 2 or 10 μM BIX and at 2 to 12 h after treatment with 50 μM BIX. Data are shown as mean ± SE ($n = 3$ or 4). $^*P < 0.05$, $^{**}P < 0.01$ versus 0 μM (**A** and **B**) or 0 μM/0 h (**C**).

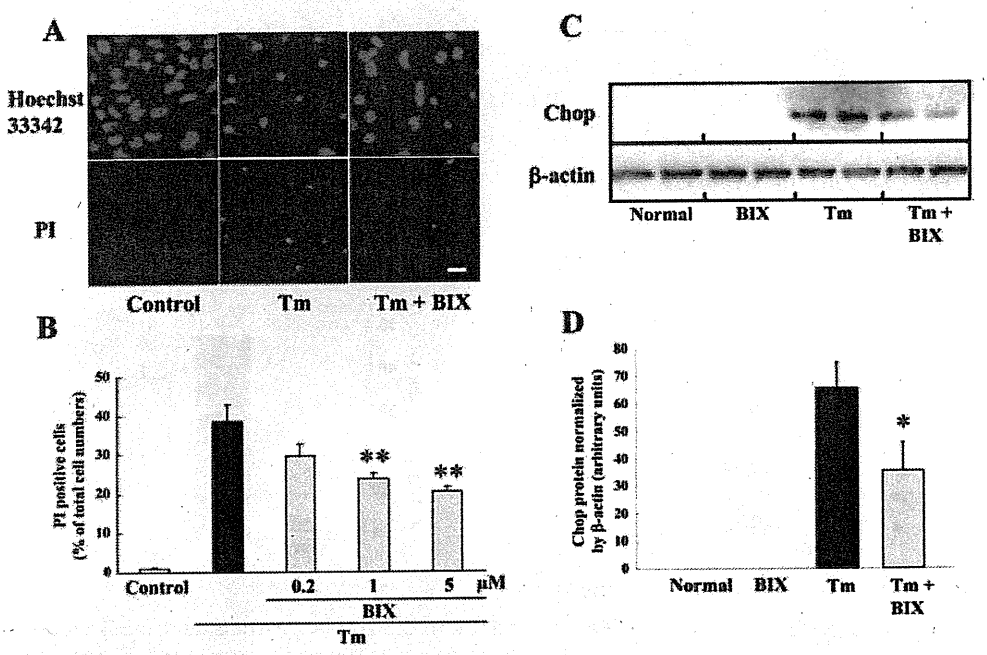

FIGURE 3. Effects of BIX on tunicamycin-induced cell death and CHOP protein expression in RGC-5 cells. (**A**) RGC-5 cells were pretreated with vehicle or with 1 μM BIX for 12 h, and then immersed in fresh medium (control) or in medium supplemented with 2 μg/mL tunicamycin (Tm; labeled Tm or Tm + BIX). *Upper* photomicrographs show Hoechst 33342 and *lower* ones propidium iodide (PI) staining at 48 h after tunicamycin stimulation. Scale bar represents 25 μm. (**B**) Numbers of PI-positive cells after tunicamycin treatment. Pretreatment of cells with BIX (1 and 5 μM) significantly reduced the amount of cell death (vs. cells treated with tunicamycin alone). (**C**) Immunoblot of CHOP protein shows that tunicamycin induced significant CHOP expression, and that pretreatment of cells with BIX at 5 μM reduced this expression with no change in the level of β-actin. *Upper panel* shows CHOP and *lower panel* shows β-actin. (**D**) Quantitative representations of β-actin-based tunicamycin-induced CHOP protein expression (in arbitrary units). Data are shown as mean ± SE (n = 6 or 8). $^*P < 0.05$, $^{**}P < 0.01$ versus tunicamycin alone.

hand, tunicamycin markedly induced CHOP protein, while pretreatment with BIX at 5 μM reduced this expression to almost half the value seen after tunicamycin treatment alone (Figs. 3C, 3D).

Effects of BIX on Cell Damage Induced by Staurosporine in RGC-5 Culture

To investigate whether BIX protects non-ER stress-induced cell death, we examined staurosporine-induced cell death. Staurosporine at 30 nM for 24 h reduced cell viability to approximately 60% of control (Fig. 4). There was no statistical difference between BIX (1 and 5 μM)-treated and vehicle-treated group.

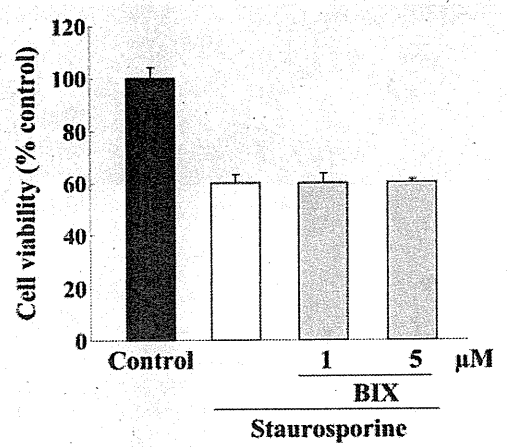

FIGURE 4. Effect of BIX on the cell death induced by staurosporine in RGC-5. RGC-5 cells were pretreated with vehicle or with BIX (1 or 5 μM) for 12 h, and then immersed in fresh medium (control) or in medium supplemented with staurosporine at 30 nM. At the end of this culture period, cell death was assessed by WST-8 assay (Cell Counting Kit-8; Dojin Kagaku). Data are shown as mean ± SE (n = 6).

BiP Protein in the Mouse Retina Induced by Intravitreous Injection of BIX

Compared with that in the nontreated retina, BiP protein expression in GCL and IPL was significantly increased at 6 and 12 h after intravitreal injection of BIX (5 nmol; Figs. 5A, 5B). Optical density analysis confirmed that administration of BIX induced BiP protein in vivo (Fig. 5D).

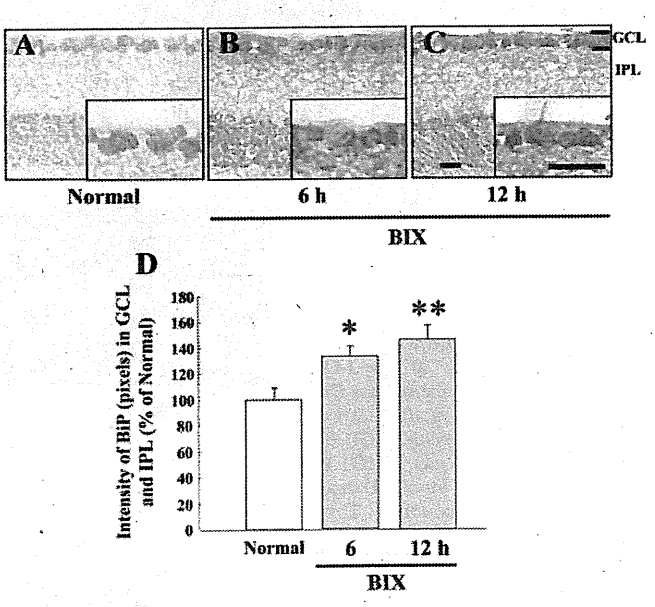

FIGURE 5. BiP protein expression in the mouse retina induced by intravitreous injection of BIX. Immunostaining probed with an antibody against BiP/GRP78. (**A**) Nontreated, (**B**) 6 h, and (**C**) 12 h after intravitreous injection of BIX (5 nmol). (**D**) Expression ratio for BiP induction intravitreous injection of BIX is represented as the ratio of intensity values. Data are shown as mean ± SE (n = 6). $^*P < 0.05$, $^{**}P < 0.01$ versus nontreated normal retina. Each scale bar represents 25 μm.

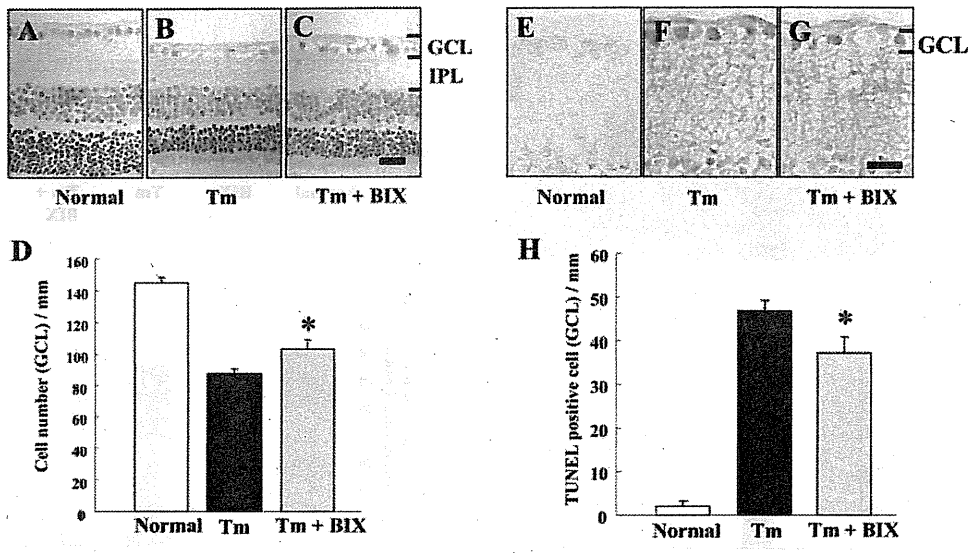

FIGURE 6. Effects of BIX on retinal damage induced by intravitreal injection of tunicamycin in mice. Hematoxylin and eosin staining of cross-sections of (**A**) nontreated, (**B**) Tm-treated, and (**C**) Tm plus BIX-treated mouse retinas at seven days after intravitreal injection of tunicamycin (1 μg) either alone or with BIX (5 nmol). (**D**) Damage was evaluated by counting cell numbers in GCL at seven days after the above injections. TUNEL staining of cross-sections of (**E**) nontreated, (**F**) Tm-treated, and (**G**) Tm plus BIX-treated mouse retinas at seven days after the above injections. (**H**) Effect of BIX on Tm-induced expression of TUNEL-positive cells at 24 h after the above injections. Data are shown as mean ± SE (n = 9 or 10). *P < 0.05 versus tunicamycin alone. Scale bars each represent 25 μm.

Protective Effect of BIX against Tunicamycin-Induced Retinal Damage in Mice

Tunicamycin decreased the cell number in GCL at 7 days after its intravitreal injection (vs. nontreated retinas; Figs. 6A, 6B). There was significantly less cell loss in GCL when BIX (5 nmol) was co-administered with the tunicamycin (Figs. 6B–6D). In addition, intravitreal injection of tunicamycin increased the number of TUNEL-positive cells in GCL at 24 h (vs. nontreated retinas; Figs. 6E, 6F). BIX (5 nmol), when co-administered with the tunicamycin, significantly reduced the number of TUNEL-positive cells (vs. tunicamycin alone; Figs. 6F–6H).

Protective Effect of BIX against Tunicamycin-Induced Retinal Damage in Thy-1-CFP Transgenic Mice

In this experiment on Thy-1-CFP transgenic mice, we confirmed the effect of BIX in a larger retinal area than that evaluated in Figure 6D. We counted the number of Thy-1-CFP-positive cells (in flatmounts) in the four white areas shown 1 mm from the center of the optic disc in Figure 7E, and then totaled these values. In the Thy-1-CFP-transgenic mouse retina, axonal fibers were evenly and densely distributed. There were congested CFP-positive cells in the vehicle-treated retina (Fig. 7A), and no change was observed in BIX-treated retinas without tunicamycin treatment (Fig. 7B). Intravitreal injection of tunicamycin decreased the Thy-1-CFP-positive cell count at 7 days (vs. vehicle-treated retina; Figs. 7A, 7C). BIX at 5 nmol, when co-administered with the tunicamycin, significantly inhibited this cell loss (Figs. 7C, 7D, 7F).

Effect of BIX on Tunicamycin-Induced CHOP Expression in Mice

Representative photograph of a nontreated retina is shown in Figure 8A. No change was observed in the BIX-treated retina (Fig. 8B). Optical density analysis of CHOP protein immunoreactivity in GCL and IPL showed that intravitreal injection of tunicamycin (1 μg) significantly increased the level of CHOP protein at 72 h after the injection (Fig. 8C). BIX (5 nmol), when co-administered with the tunicamycin, significantly inhibited this effect (Figs. 8D, 8E).

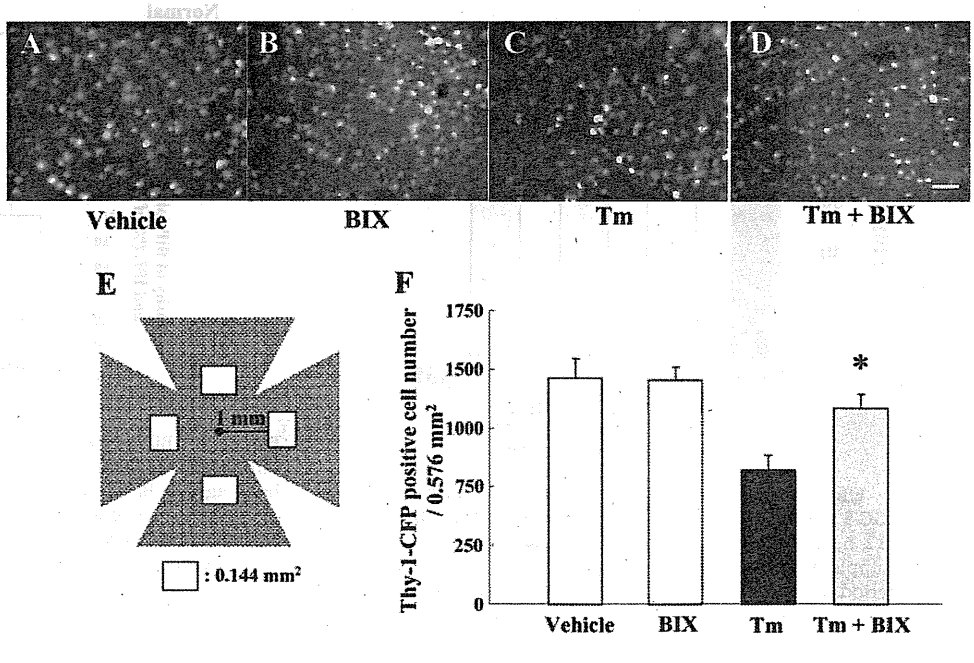

FIGURE 7. Effects of BIX on retinal damage induced by intravitreal injection of tunicamycin in Thy-1-CFP transgenic mice. Mouse retinas (flatmounts) at seven days after intravitreal injection of (**A**) vehicle, (**B**) BIX (5 nmol), (**C**) Tm (1 μg), or (**D**) Tm (1 μg) plus BIX (5 nmol). Damage was evaluated by counting Thy-1-CFP-positive cell numbers in the four *white* areas shown in (**E**) (each area 0.144 mm^2 × 4 areas; total 0.576 mm^2) at seven days after the above intravitreal injections. (**F**) Effect of BIX against Tm-induced damage (indicated by decreased number of Thy-1-CFP-positive cells) at seven days after intravitreal injection. Data are shown as mean ± SE (n = 9 or 10). *P < 0.05 versus tunicamycin alone. Scale bar represents 25 μm.

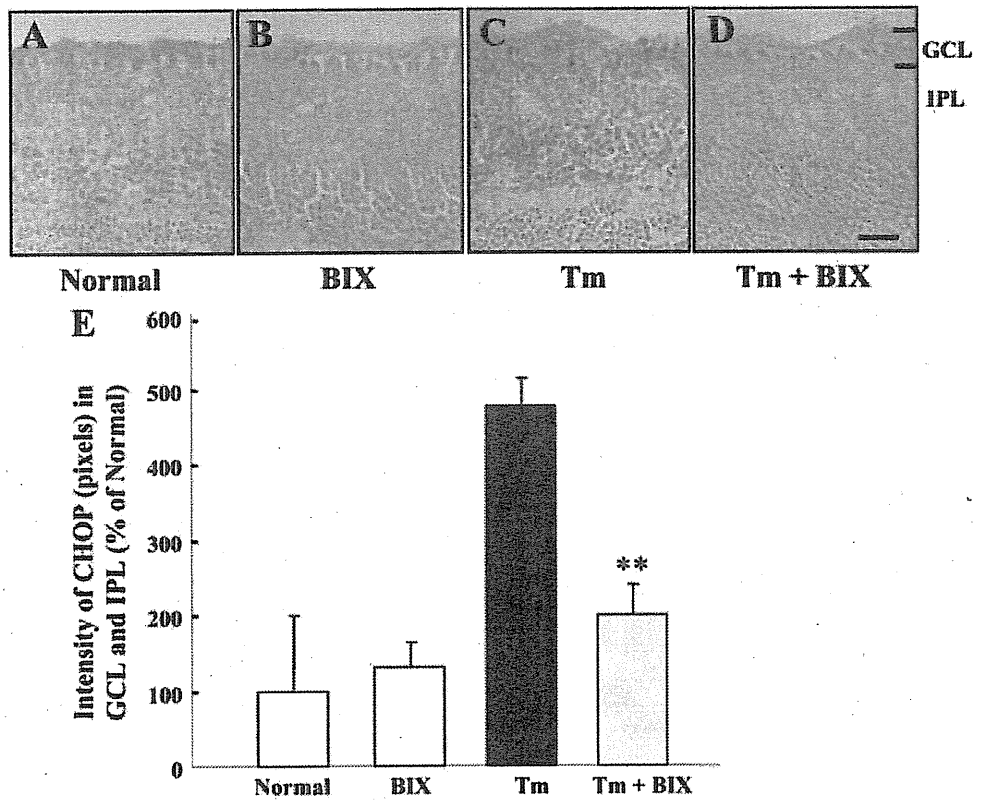

FIGURE 8. Effect of BIX on tunicamycin-induced CHOP expression in the mouse retina. Mouse retinas (cross-sections) either (A) nontreated or at three days after intravitreal injection of (B) BIX (5 nmol), (C) Tm (1 μg) or (D) Tm (1 μg) plus BIX (5 nmol). (E) Relative density of CHOP protein expression in GCL and IPL at three days after the above intravitreal injections. Data are shown as mean ± SE ($n = 6$). $^{**}P < 0.01$ versus tunicamycin alone. Scale bar represents 25 μm.

Effect of BIX on Tunicamycin-Induced XBP-1 Expression in ERAI Mice

In ERAI mice, the fluorescence intensity arising from the XBP-1-venus fusion protein (indicating ER stress activation) can be easily visualized, allowing evaluation of the effect of ER stress on the retina. In the representative photographs of flatmount retinas from ERAI mice shown in Figure 9, no difference was observed between vehicle-treated and BIX-treated retinas (Fig. 9B). Intravitreal injection of tunicamycin (1 μg) induced XBP-1-venus expression (vs. the vehicle-treated retina; Fig. 9C). Immunoblot analysis of XBP-1-venus protein expression in the retina (using an anti-GFP antibody) showed that intravitreal injection of tunicamycin (1 μg) significantly raised the level of XBP-1-venus protein, and that BIX (5 nmol), when co-administered with the tunicamycin (Fig. 9D), significantly inhibited this effect (Figs. 9E, 9F).

Protective Effect of BIX against NMDA-Induced Retinal Damage in Mice

A representative photograph of a nontreated retina is shown in Figure 10A. Intravitreal injection of NMDA (a) decreased the

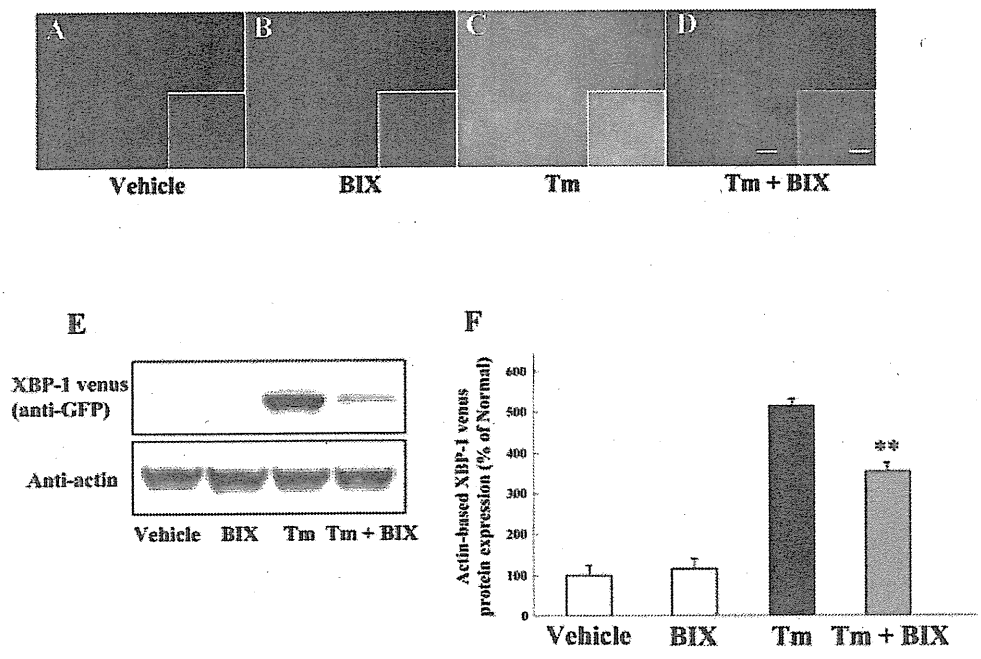

FIGURE 9. Effect of BIX on tunicamycin-induced XBP-1 venus expression in ERAI mice. Mouse retinas (flatmounts) at 24 h after intravitreal injection of (A) vehicle, (B) BIX (5 nmol), (C) Tm (1 μg) or (D) Tm (1 μg) plus BIX (5 nmol). (E) *Upper panel* shows XBP-1 venus protein expression, while *lower panel* shows β-actin protein expression at 24 h after the above injections. (F) Western blot analysis showing effect of BIX on Tm-induced expression of β-actin-based XBP-1 venus protein expression at 24 h after the above injections. Data are shown as mean ± SE ($n = 8$). $^{*}P < 0.01$ versus tunicamycin alone. Scale bars in main photomicrographs and in *insets* represent 25 and 5 μm, respectively.

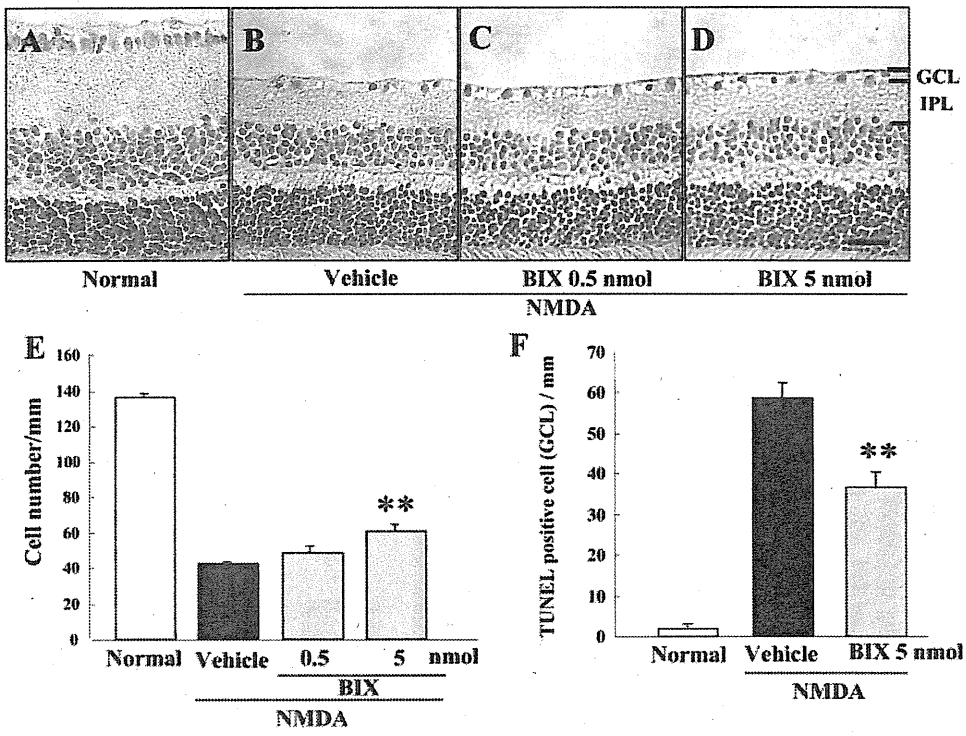

FIGURE 10. Effects of BIX on retinal damage induced by intravitreal injection of NMDA in mice. Mouse retinas (cross-sections) either (**A**) nontreated or at seven days after intravitreal injection of (**B**) NMDA (40 nmol) alone or (**C**, **D**) NMDA (40 nmol) plus BIX (0.5 or 5 nmol). (**E**) Damage was evaluated by counting cell numbers in GCL at seven days after the above intravitreal injections. (**F**) Effect of BIX on NMDA-induced expression of TUNEL-positive cells at 24 h after intravitreal injection of NMDA (40 nmol) either alone or with BIX (5 nmol). Data are shown as mean ± SE ($n = 9$ or 10). $^{**}P < 0.01$ versus NMDA-treated control group. Scale bar represents 25 μm.

cell number in GCL at 7 days (Figs. 10B, 10E) and (b) increased the number of TUNEL-positive cells in GCL at 24 h (vs. nontreated normal retina; Fig. 10F). BIX (5 nmol), when co-administered with the NMDA, significantly reduced (vs. NMDA alone) both the cell loss in GCL (Figs. 10D, 10E) and the number of TUNEL-positive cells (Fig. 10F). On the other hand, there was no statistical difference between BIX (0.5 nmol)- and vehicle-treated group in NMDA-induced cell death in GCL (Figs. 10C, 10E).

Effect of BIX on NMDA-Induced CHOP Expression in Mice

A representative photograph of a nontreated retina is shown in Figure 11A and no change was detected between nontreated

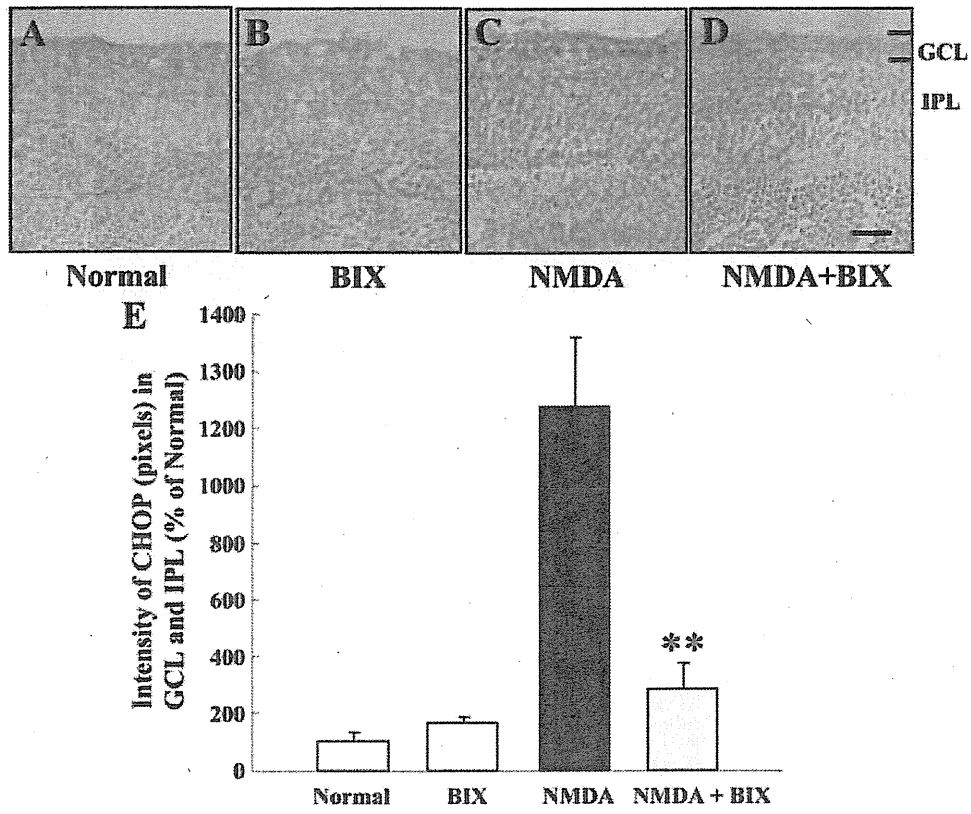

FIGURE 11. Effect of BIX on NMDA-induced CHOP expression in mice. Mouse retinas (cross-sections) either (**A**) nontreated or at three days after intravitreal injection of (**B**) NMDA (40 nmol) alone or (**C**) NMDA (40 nmol), or (**D**) NMDA (40 nmol) plus BIX (5 nmol). (**E**) Relative density of CHOP protein expression in GCL and IPL at three days after the above intravitreal injections. Data are shown as mean ± SE ($n = 6$). $^{**}P < 0.01$ versus NMDA alone. Scale bar represents 25 μm.

retina and the BIX-treated retina without NMDA treatment (Figs. 11A, 11B). Optical density analysis of CHOP protein immunoreactivity in GCL and IPL showed that intravitreal injection of NMDA (40 nmol) significantly increased the level of CHOP protein at 72 h after the injection (Fig. 11C). When co-administered with the NMDA, BIX (5 nmol) significantly inhibited this effect (Figs. 11D, 11E).

Discussion

In the present study, we confirmed that BIX preferentially induces BiP mRNA in RGC-5. Although it also induced GRP94, calreticulin, $p58^{IPK}$, and ASNS, these inductions were lower than that of BiP. This is consistent with our previous study that BIX preferentially induced BiP with slight inductions of GRP94, calreticulin, and CHOP mediated by the activating transcription factor 6 (ATF6) pathway accompanied by activation of ERSEs, and that BIX does not affect the pathway downstream of IRE1 or the translational control branch downstream of PERK in SK-N-SH cells.[32] Therefore, BIX is not just an ER stressor such as tunicamycin or thapsigargin, and we consider that the induction of BiP by BIX is mediated by the ATF6 pathway in RGC-5 similar to that in SK-N-SH cells. Next, we evaluated the effects of BIX, as a preferential inducer of BiP, on ER stress-induced in vitro cell death in RGC-5 (a rat ganglion cell-line) and in vivo retinal damage in mice. We found that BIX reduced tunicamycin-induced cell death in RGC-5 and also reduced both tunicamycin-induced and NMDA-induced retinal damage in mice. Our previous study revealed that BIX (a) reduced tunicamycin-induced cell death in SK-N-SH cells, (b) contributed to the induction of BiP expression via the ATF-6 pathway (but not via the PERK or IRE1 pathways), and (c) on intracerebroventricular injection, prevented the neuronal damage induced by focal ischemia in mice.[32] Furthermore, immunostaining revealed that intravitreal injection of BIX significantly induced BiP protein in mouse retina. Particularly, it expressed in GCL and IPL (versus both the normal and the sham retina). On the other hand, there was little protective effect of BIX against RGC-5 damages after staurosporine treatment. Staurosporine is well known as a nonspecific inhibitor of protein kinases and initiates caspase-dependent apoptosis in many cell types.[41,42] Our previous studies revealed that staurosporine induced cell death without any changes in the expression of BiP or CHOP protein.[12,43] Furthermore, preliminary study showed that treatment with BIX (1 and 5 μM) did not inhibit RGC-5 cell death 48 h after serum deprivation, which does not induce any UPR-responses such as BiP or CHOP (unpublished data). These results strongly support that BIX selectively protects cell damage induced by ER stress.

Recently, we reported that in mice, increased expressions of XBP-1 splicing, BiP, and CHOP could be detected after the induction of retinal damage by tunicamycin, NMDA, or an elevation of intraocular pressure.[13] That report was the first to demonstrate an involvement of ER stress and BiP in retinal cell death in mice. Hence, in the present study we asked whether BIX can prevent such retinal damage. By histologic analysis and TUNEL staining, we estimated that BIX reduced tunicamycin-induced retinal damage in GCL. However, the cell counts in partial cross sections provide a comparatively small sample on which quantitative morphometry can be used to judge such an effect. Therefore, we used Thy-1-CFP transgenic mice[36] to examine the effect of BIX in a large retinal area. This transgene contains a CFP gene under the direction of regulatory elements derived from the mouse Thy-1 gene, and the transgenic mice express CFP protein in RGC and in the inner part of the IPL of the retina.[36] Our results show that BIX exerted a protective effect against tunicamycin-induced retinal damage in the Thy-1-CFP transgenic mouse. However, it is possible that microglial cells become co-labeled with CFP by phagocytosis of the dying RGCs. In this study, we evaluated CFP-positive cells in 7 days after tunicamycin injection. In our previous and preliminary studies, activated microglia cells in GCL were increased at 3 days after NMDA injection[13] and their increases were almost ceased within the 7 days (unpublished data). Furthermore, microglial cells can be distinguished with neuronal cells by their morphologic features.[44] In fact, microglial cells were scarcely observed at seven days after tunicamycin injection, similar to that at seven days after NMDA injection. When we investigated the effect of BIX on NMDA-induced retinal damage in ddY mice, we found that it significantly attenuated such damage. NMDA is well known to induce RGC death and optic-nerve loss (effects mediated by excitatory glutamate receptor), and such neuronal death is believed to play a role in many neurologic and neurodegenerative diseases.[45,46] Recently, Uehara et al.[47] noted that mild exposure to NMDA induced apoptotic cell death in primary cortical culture, and they demonstrated this effect to be caused by an accumulation of polyubiquitinated proteins and increases in XBP-1 mRNA splicing and CHOP mRNA (reflecting activation of the UPR signaling pathway). They also found that protein-disulphide isomerase, which assists in the maturation and transport of unfolded secretory proteins, prevented the neurotoxicity associated with ER stress. These findings suggested that activation of ER stress may participate in the retinal cell death occurring after NMDA-receptor activation and/or an ischemic insult.[47]

In our investigation of the mechanisms underlying the above-mentioned effects, we focused on CHOP. Since CHOP is a member of the CCAAT/enhancer-binding protein family that is induced by ER stress and participates in ER-mediated apoptosis, CHOP may be a key molecule in retinal cell death.[48] We found that treatment with tunicamycin induced apoptotic cell death in RGC-5 and also induced a production of ER stress-related proteins (BiP, the phosphorylated form of eIF2α, and CHOP protein). BIX reduced both the cell death and the CHOP protein expression induced by tunicamycin in RGC-5 in vitro. BIX also attenuated the CHOP protein expression induced by either tunicamycin or NMDA in the mouse retina in vivo. As mentioned above, BIX may affect CHOP protein expression through ATF6 pathway, but no change was observed in BIX-treated RGC-5. In our previous data in SK-N-SH cells, BIX slightly increased CHOP mRNA only at 2 h after the treatment. Expression of CHOP is mainly regulated by three transcription factors—ATF4, cleaved ATF6, and x-box binding protein-1 (XBP-1)—which are downstream effectors during ER stress in similar to other ER chaperones. These differences between BiP and CHOP expression by BIX may be due to the difference of their promoters. CHOP promoter contains at least two ERSE motifs (CHOP ERSE-1 and CHOP ERSE-2) located in opposite directions with a 9 bp overlap, and one of ERSEs is inactive.[49] On the other hand, BiP promoter has three functional ERSE motifs of the rat GRP78 promoter (ERSE-163, ERSE-131, and ERSE-98).[50] These variations in each promoter may contribute to the differences among the expressions of ER chaperons induced by BIX and the lack of CHOP expression.

Subsequently, we monitored XBP-1 activation in the mouse retina in vivo, using ERAI transgenic mice.[37] Effective identification of cells under ER stress conditions is possible in the retina in these mice, as described in our previous report.[13] Here, ERAI mice carrying the F-XBP1ΔDBD-venus expression gene were used to monitor ER stress. The fluorescence intensity arising from the X-box binding protein (XBP1)-venus fusion protein, indicating ER stress activation, was increased in cells within GCL and IPL at 24 h after injection of tunicamycin into the vitreous. BIX significantly reduced this expression, indicating that BIX may attenuate the retinal damage induced

by ER stress-associated factors. In our previous study,[32] we found that BIX induced BiP protein expression via the ATF-6 pathway (not via other ER stress-associated factors such as the PERK and IRE1 pathways) in SK-N-SH cells. Possibly, the protective mechanism underlying the effect of BIX on the mouse retina may be the same as that revealed by our previous study, but further experiments will be needed to clarify this issue.

In conclusion, we have demonstrated that BIX, a preferential inducer of BiP, inhibits both the neuronal cell death induced by ER stress in vitro in RGC-5 cells and in vivo in the mouse retina. Hence, an increase in BiP might be one of the targets of mechanisms bestowing neuroprotection in retinal diseases.

Acknowledgments

The authors thank Masayuki Miura (Department of Genetics, Graduate School of Pharmaceutical Sciences, University of Tokyo, Tokyo, Japan) for the kind gift of ERAI mice, and Rumi Uchibayashi and Shunsake Imai for technical assistance.

References

1. Travers KJ, Patil CK, Wodicka L, Lockhart DJ, Weissman JS, Walter P. Functional and genomic analyses reveal an essential coordination between the unfolded protein response and ER-associated degradation. *Cell.* 2000;101:249-258.
2. Harding HP, Novoa I, Zhang Y, et al. Regulated translation initiation controls stress-induced gene expression in mammalian cells. *Mol Cell.* 2000;6:1099-1108.
3. Schroder M, Kaufman RJ. The mammalian unfolded protein response. *Annu Rev Biochem.* 2005;74:739-789.
4. Katayama T, Imaizumi K, Honda A, et al. Disturbed activation of endoplasmic reticulum stress transducers by familial Alzheimer's disease-linked presenilin-1 mutations. *J Biol Chem.* 2001;276:43446-43454.
5. Ryu EJ, Harding HP, Angelastro JM, Vitolo OV, Ron D, Greene LA. Endoplasmic reticulum stress and the unfolded protein response in cellular models of Parkinson's disease. *J Neurosci.* 2002;22:10690-10698.
6. Oyadomari S, Koizumi A, Takeda K, et al. Targeted disruption of the Chop gene delays endoplasmic reticulum stress-mediated diabetes. *J Clin Invest.* 2002;109:525-532.
7. Roybal CN, Yang S, Sun CW, et al. Homocysteine increases the expression of vascular endothelial growth factor by a mechanism involving endoplasmic reticulum stress and transcription factor ATF4. *J Biol Chem.* 2004;279:14844-14852.
8. Rebello G, Ramesar R, Vorster A, et al. Apoptosis-inducing signal sequence mutation in carbonic anhydrase IV identified in patients with the RP17 form of retinitis pigmentosa. *Proc Natl Acad Sci USA.* 2004;101:6617-6622.
9. Lin JH, Li H, Yasumura D, et al. IRE1 signaling affects cell fate during the unfolded protein response. *Science.* 2007;318:944-949.
10. Joe MK, Sohn S, Hur W, Moon Y, Choi YR, Kee C. Accumulation of mutant myocilins in ER leads to ER stress and potential cytotoxicity in human trabecular meshwork cells. *Biochem Biophys Res Commun.* 2003;312:592-600.
11. Gould DB, Marchant JK, Savinova OV, Smith RS, John SW. Col4a1 mutation causes endoplasmic reticulum stress and genetically modifiable ocular dysgenesis. *Hum Mol Genet.* 2007;16:798-807.
12. Shimazawa M, Ito Y, Inokuchi Y, Hara H. Involvement of double-stranded RNA-dependent protein kinase in ER stress-induced retinal neuron damage. *Invest Ophthalmol Vis Sci.* 2007;48:3729-3736.
13. Shimazawa M, Inokuchi Y, Ito Y, et al. Involvement of ER stress in retinal cell death. *Mol Vis.* 2007;13:578-587.
14. Mahoney WC, Duksin D. Biological activities of the two major components of tunicamycin. *J Biol Chem.* 1979;254:6572-6576.
15. Awai M, Koga T, Inomata Y, et al. NMDA-induced retinal injury is mediated by an endoplasmic reticulum stress-related protein, CHOP/GADD153. *J Neurochem.* 2006;96:43-52.
16. Lee YK, Brewer JW, Hellman R, Hendershot LM. BiP and immunoglobulin light chain cooperate to control the folding of heavy chain and ensure the fidelity of immunoglobulin assembly. *Mol Biol Cell.* 1999;10:2209-2219.
17. Li WW, Alexandre S, Cao X, Lee AS. Transactivation of the grp78 promoter by Ca^{2+} depletion. A comparative analysis with A23187 and the endoplasmic reticulum Ca^{2+}-ATPase inhibitor thapsigargin. *J Biol Chem.* 1993;268:12003-12009.
18. van de Put FH, Elliott AC. The endoplasmic reticulum can act as a functional Ca^{2+} store in all subcellular regions of the pancreatic acinar cell. *J Biol Chem.* 1997;272:27764-27770.
19. Lievremont JP, Rizzuto R, Hendershot L, Meldolesi J. BiP, a major chaperone protein of the endoplasmic reticulum lumen, plays a direct and important role in the storage of the rapidly exchanging pool of Ca^{2+}. *J Biol Chem.* 1997;272:30873-30879.
20. Helenius A. How N-linked oligosaccharides affect glycoprotein folding in the endoplasmic reticulum. *Mol Biol Cell.* 1994;5:253-265.
21. Kuznetsov G, Chen LB, Nigam SK. Multiple molecular chaperones complex with misfolded large oligomeric glycoproteins in the endoplasmic reticulum. *J Biol Chem.* 1997;272:3057-3063.
22. Klausner RD, Sitia R. Protein degradation in the endoplasmic reticulum. *Cell.* 1990;62:611-614.
23. Blond-Elguindi S, Cwirla SE, Dower WJ, et al. Affinity panning of a library of peptides displayed on bacteriophages reveals the binding specificity of BiP. *Cell.* 1993;75:717-728.
24. Knarr G, Gething MJ, Modrow S, Buchner J. BiP binding sequences in antibodies. *J Biol Chem.* 1995;270:27589-27594.
25. Knarr G, Modrow S, Todd A, Gething MJ, Buchner J. BiP-binding sequences in HIV gp160. Implications for the binding specificity of bip. *J Biol Chem.* 1999;274:29850-29857.
26. Brodsky JL, Werner ED, Dubas ME, Goeckeler JL, Kruse KB, McCracken AA. The requirement for molecular chaperones during endoplasmic reticulum-associated protein degradation demonstrates that protein export and import are mechanistically distinct. *J Biol Chem.* 1999;274:3453-3460.
27. Meerovitch K, Wing S, Goltzman D. Proparathyroid hormone-related protein is associated with the chaperone protein BiP and undergoes proteasome-mediated degradation. *J Biol Chem.* 1998;273:21025-21030.
28. Katayama T, Imaizumi K, Sato N, et al. Presenilin-1 mutations downregulate the signalling pathway of the unfolded-protein response. *Nat Cell Biol.* 1999;1:479-485.
29. Yu Z, Luo H, Fu W, Mattson MP. The endoplasmic reticulum stress-responsive protein GRP78 protects neurons against excitotoxicity and apoptosis: suppression of oxidative stress and stabilization of calcium homeostasis. *Exp Neurol.* 1999;155:302-314.
30. Rao RV, Peel A, Logvinova A, et al. Coupling endoplasmic reticulum stress to the cell death program: role of the ER chaperone GRP78. *FEBS Lett.* 2002;514:122-128.
31. Reddy RK, Mao C, Baumeister P, Austin RC, Kaufman RJ, Lee AS. Endoplasmic reticulum chaperone protein GRP78 protects cells from apoptosis induced by topoisomerase inhibitors: role of ATP binding site in suppression of caspase-7 activation. *J Biol Chem.* 2003;278:20915-20924.
32. Kudo T, Kanemoto S, Hara H, et al. A molecular chaperone inducer protects neurons from ER stress. *Cell Death Differ.* 2008;15:364-375.
33. Krishnamoorthy RR, Agarwal P, Prasanna G, et al. Characterization of a transformed rat retinal ganglion cell line. *Brain Res Mol Brain Res.* 2001;86:1-12.
34. Chen D, Padiernos E, Ding F, Lossos IS, Lopez CD. Apoptosis-stimulating protein of p53-2 (ASPP2/53BP2L) is an E2F target gene. *Cell Death Differ.* 2005;12:358-368.
35. Jiang Y, Ahn EY, Ryu SH, et al. Cytotoxicity of psammaplin A from a two-sponge association may correlate with the inhibition of DNA replication. *BMC Cancer.* 2004;4:70.
36. Feng G, Mellor RH, Bernstein M, et al. Imaging neuronal subsets in transgenic mice expressing multiple spectral variants of GFP. *Neuron.* 2000;28:41-51.
37. Iwawaki T, Akai R, Kohno K, Miura M. A transgenic mouse model for monitoring endoplasmic reticulum stress. *Nat Med.* 2004;10:98-102.

38. Siliprandi R, Canella R, Carmignoto G, et al. N-methyl-D-aspartate-induced neurotoxicity in the adult rat retina. *Vis Neurosci.* 1992; 8:567–573.
39. Jeon CJ, Strettoi E, Masland RH. The major cell populations of the mouse retina. *J Neurosci.* 1998;18:8936–8946.
40. Onozuka T, Sawamura D, Goto M, Yokota K, Shimizu H. Possible role of endoplasmic reticulum stress in the pathogenesis of Darier's disease. *J Dermatol Sci.* 2006;41:217–220.
41. Weil M, Jacobson MD, Coles HS, et al. Constitutive expression of the machinery for programmed cell death. *J Cell Biol.* 1996;133: 1053–1059.
42. Taylor J, Gatchalian CL, Keen G, Rubin LL. Apoptosis in cerebellar granule neurones: involvement of interleukin-1 beta converting enzyme-like proteases. *J Neurochem.* 1997;68:1598–1605.
43. Inokuchi Y, Shimazawa M, Nakajima Y, Suemori S, Mishima S, Hara H. Brazilian green propolis protects against retinal damage in vitro and in vivo. *Evid Based Complement Alternat Med.* 2006;3:71–77.
44. Chidlow G, Wood JP, Manavis J, Osborne NN, Casson RJ. Expression of osteopontin in the rat retina: effects of excitotoxic and ischemic injuries. *Invest Ophthalmol Vis Sci.* 2008;49:762–771.
45. Sucher NJ, Lipton SA, Dreyer EB. Molecular basis of glutamate toxicity in retinal ganglion cells. *Vision Res.* 1997;37:3483–3493.
46. Henneberry RC, Novelli A, Cox JA, Lysko PG. Neurotoxicity at the N-methyl-D-aspartate receptor in energy-compromised neurons. An hypothesis for cell death in aging and disease. *Ann NY Acad Sci.* 1989;568:225–233.
47. Uehara T, Nakamura T, Yao D, et al. S-nitrosylated protein-disulphide isomerase links protein misfolding to neurodegeneration. *Nature.* 2006;441:513–517.
48. Wang XZ, Lawson B, Brewer JW, et al. Signals from the stressed endoplasmic reticulum induce C/EBP-homologous protein (CHOP/GADD153). *Mol Cell Biol.* 1996;16:4273–4280.
49. Ubeda M, Habener JF. CHOP gene expression in response to endoplasmic-reticular stress requires NFY interaction with different domains of a conserved DNA-binding element. *Nucleic Acids Res.* 2000;28:4987–4997.
50. Foti DM, Welihinda A, Kaufman RJ, Lee AS. Conservation and divergence of the yeast and mammalian unfolded protein response. Activation of specific mammalian endoplasmic reticulum stress element of the grp78/BiP promoter by yeast Hac1. *J Biol Chem.* 1999;274:30402–30409.

Neuroscience Letters 484 (2010) 43–46

Contents lists available at ScienceDirect

Neuroscience Letters

journal homepage: www.elsevier.com/locate/neulet

Post-treatment of a BiP inducer prevents cell death after middle cerebral artery occlusion in mice

Yasuhisa Oida[a,b], Junya Hamanaka[a], Kana Hyakkoku[a], Masamitsu Shimazawa[a], Takashi Kudo[c], Kazunori Imaizumi[d], Tadashi Yasuda[b], Hideaki Hara[a,*]

[a] Molecular Pharmacology, Department of Biofunctional Evaluation, Gifu Pharmaceutical University, 1-25-4 Daigaku-nishi, Gifu 501-1196, Japan
[b] Department of Pharmacy, Ogaki Municipal Hospital, Gifu 503-8502, Japan
[c] Department of Clinical Neuroscience, Psychiatry, Graduate School of Medicine, Osaka University, Osaka 565-0871, Japan
[d] Department of Biochemistry, Division of Genome Radiobiology and Medical Science, Graduate School of Biomedical Science, Hiroshima University 1-2-3, Kasumi, Minami-ku, Hiroshima 734-8551, Japan

ARTICLE INFO

Article history:
Received 25 May 2010
Received in revised form 3 August 2010
Accepted 6 August 2010

Keywords:
Apoptosis
ER stress
Immunoglobulin heavy chain binding protein (BiP)
Ischemia
Mouse

ABSTRACT

We previously reported the effect of a selective inducer of BiP (a BiP inducer X; BIX) after permanent middle cerebral artery occlusion (MCAO) in mice. However, in acute stroke, almost all drugs have been used clinically after the onset of events. We evaluated the effect of post-treatment of BIX after permanent MCAO in mice, and examined its neuroprotective properties in *in vivo* mechanism. BIX (intracerebroventricular injection at 20 μg) administered either at 5 min or 3 h after occlusion reduced both infarct volume and brain swelling, but at 6 h after occlusion there was no reduction. BIX protected against the decrease in a dose-dependent manner. Furthermore, BIX reduced the number of terminal deoxynucleotidyl transferase-mediated dUTP nick end-labeling (TUNEL)-positive cells induced by the ischemia in ischemic penumbra. These findings indicate that post-treatment with BIX after ischemia has neuroprotective effects against acute ischemic neuronal damage in mice even when given up to 3 h after MCAO. BIX may therefore be a potential drug for stroke.

Stroke is the third most common cause of death after heart attack and cancer, and it has profound negative social and economic effects. The only preventive treatment for stroke is anti-platelet therapy for patients with transient ischemic attack or stroke, which produces a modest but clinically worthwhile benefit [3]. In acute stroke, only a small fraction of patients benefit from intravenous administration of recombinant tissue plasminogen activator (t-PA), which is the only drug with proven effectiveness in reducing the size of infarct in humans [1,17].

BiP is one of the molecular chaperones localized to the ER membrane, and is a highly conserved member of the 70-kDa heat shock protein family [10,11]. It has been reported that the expression of BiP, an endoplasmic reticulum (ER) molecular chaperone, was upregulated by ischemia in focal and global transient ischemia models [7,16,19]. Furthermore, previous reports showed that the induction of BiP prevents neuronal death induced by ER stress [8,14,15,21]. By contrast, inhibition of GRP78 (78 kDa glucose-regulated protein) mRNA induction increases cell death in response to calcium release from the ER, oxidative stress, hypoxia, and T-cell-mediated cytotoxicity [4,13,18]. Therefore, BiP activators will be effective agents against cerebral ischemia.

ER stress, which is caused by an accumulation of unfolded proteins in the ER lumen, is associated with stroke and with neurodegenerative diseases such as Parkinson's and Alzheimer's. An earlier study showed that pretreatment with BIX (intracerebroventricular injection at 5 or 20 μg) protects cells from ER stress [9]. BIX is an inducer of BiP mRNA found by using a BiP reporter assay system [9]. Our previous report showed that BIX selectively induces BiP in SK-N-SH cells and pretreatment with BIX (intracerebroventricular injection at 5 or 20 μg) reduces the area of infarction and the neuronal cell death due to focal cerebral ischemia in mice [9].

In the present study, we examined the neuroprotective effects of post-treatment with BIX on infarction, brain swelling, neurological deficits, and apoptosis in a murine permanent focal cerebral ischemia model.

The experimental designs and all procedures were in accordance with the U.S. National Institutes of Health Guide for the Care and Use of Laboratory Animals and the Animal Care Guidelines issued by the Animal Experimental Committee of Gifu Pharmaceutical University, and approved by the Animal Experimental Committee of Gifu Pharmaceutical University. All *in vivo* experiments were per-

* Corresponding author. Tel.: +81 58 230 8126; fax: +81 58 230 8126.
E-mail address: hidehara@gifu-pu.ac.jp (H. Hara).

0304-3940/$ – see front matter © 2010 Elsevier Ireland Ltd. All rights reserved.
doi:10.1016/j.neulet.2010.08.015

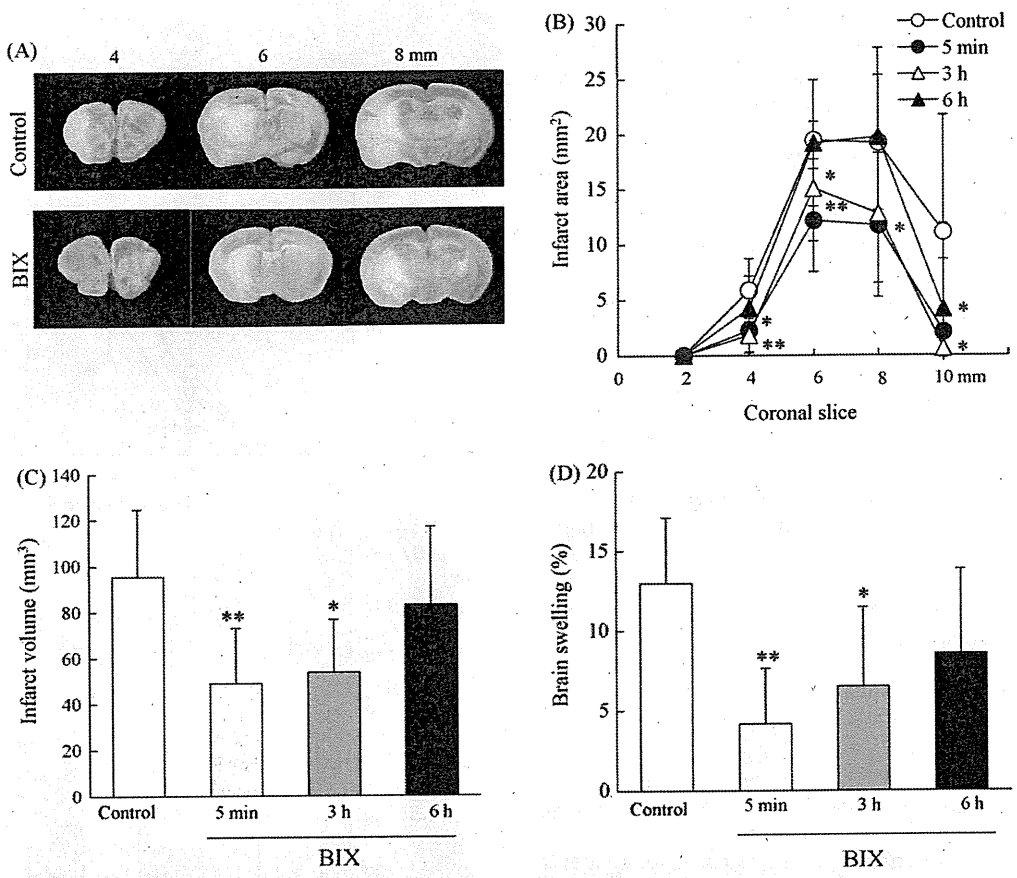

Fig. 1. Effects of BIX administered after ischemia on a therapeutic window after MCAO in mice. (A) TTC staining of coronal brain sections (2 mm thick) at 24 h after permanent MCAO in representative mice. Upper panels, vehicle-injected (control) mice. Lower panels, BIX (intracerebroventricular injection at 20 μg)-treated mice. (B) Brain infarct area measured at 24 h after MCA occlusion. Brains were removed and the forebrains sliced into five coronal 2 mm sections. $^{*}P<0.05$, $^{**}P<0.01$ vs. control ($n=7$–11). (C and D) Effects of BIX on infarct volume and brain swelling (measured at 24 h after MCAO). Values are expressed as the mean ± S.D. $^{*}P<0.05$, $^{**}P<0.01$ vs. control ($n=7$–11).

formed using male adult ddY mice (body weight 26–32 g; Japan SLC Ltd., Shizuoka, Japan). The animals were housed at 24 ± 2 °C under a 12 h light/dark cycle (lights on from 07:00 to 19:00). Each animal was used for one experiment only.

Anesthesia was induced using 2.0–3.0% isoflurane, and maintained using 1.0–1.5% isoflurane (both in 70% N_2O/30% O_2) by means of an animal general anesthesia machine (Soft Lander; Sin-ei Industry Co. Ltd., Saitama, Japan). Body temperature was maintained at 37.0–37.5 °C with the aid of a heating pad and heating lamp. After a midline skin incision, the left external carotid artery was exposed, and its branches were occluded [5,6]. An 8-0 nylon monofilament (Ethicon, Somerville, NJ, USA) coated with a mixture of silicone resin (Xantopren; Bayer Dental, Osaka, Japan) was introduced into the left internal carotid artery through the common carotid artery so as to occluded the origin of the middle cerebral artery. Then, the left common carotid artery was occluded. After the surgery, the mice were kept in the preoperative condition (room temperature; 24 ± 2 °C) until sampling.

BIX was dissolved in 10% DMSO, and fresh solution was made daily. Two microliters of vehicle (10% DMSO in saline) or BIX 1, 5 or 20 μg was administered intracerebroventricularly at 5 min, 3 h, and 6 h after ischemia. Used animals were divided into each group so as not to make significant differences in average body weight.

To analyze infarct volume, mice were euthanized using sodium pentobarbital at 24 h after MCAO, and forebrains were sectioned coronally into five slices (2 mm thick). These were placed in 2% TTC at 37 °C for 30 min. The infarcted areas and volumes were recorded as images using a digital camera (Coolpix 4500; Nikon, Tokyo, Japan), then quantified using Image J, and calculated as in our previous report [5]. Brain swelling was calculated according to the following formula: (infarct volume + ipsilateral undamaged volume − contralateral volume) × 100/contralateral volume (%) [6]. To minimize potential bias in infarct volume assessment, the investigator who analyzed the cerebral infarction was blinded.

Mice were tested for neurological deficits at 24 h after MCAO. Scoring was done as described in our previous study [6], using the following scale: (0) no observable neurological deficits (normal); (1) failure to extend the right forepaw (mild); (2) circling to the contralateral side (moderate); and (3) loss of walking or righting reflex (severe). The investigator who rated the mice was blinded as to the group to which each mouse belonged.

The terminal deoxynucleotidyl transferase-mediated dUTP nick end-labeling (TUNEL) assay was performed according to the manufacturer's instructions (Roche Molecular Biochemicals Inc., Mannheim, Germany). Ischemic areas of cortical brain sections 0.4–1.0 mm anterior to bregma (through the anterior commissure) were excised and used. The brains were removed, fixed overnight in 4% paraformaldehyde, and immersed for 1 day in 25% sucrose with phosphate-buffered saline (PBS). The brains were then embedded in a supporting medium for frozen-tissue specimens (OCT compound; Tissue-Tek). Cerebral sections 20 μm thick were cut on a cryostat at −25 °C, and stored at −80 °C until staining. After washing twice with PBS, sections were incubated with terminal deoxyribonucleotidyl transferase (TdT) enzyme at 37 °C for 1 h. The sections were washed three times in PBS for 1 min at room temperature. Sections were subsequently incubated with an anti-fluorescein antibody-peroxidase conjugate at room temperature in a humidified chamber for 30 min, and then developed using DAB tetrahydrochloride peroxidase substrate. To quantify the number of DNA-fragmented cells present after MCAO, the numbers of

TUNEL-positive cells such as necrotic and apoptotic cells) in the caudate-putamen (as the ischemic core) and cortex (as the ischemic penumbra, two areas) were counted in a high-power field (×200) on a section through the anterior commissure by a blinded investigator. Each count was expressed as number/mm^2 (n = 7).

Data are presented as the mean ± S.D. Statistical comparisons were made using a one-way ANOVA followed by Dunnett's test and Mann–Whitney U-test (using STAT VIEW version 5.0: SAS Institute, Cary, NC). $P < 0.05$ was considered to indicate statistical significance.

Using TTC staining, we examined whether BIX would reduce infarct volume. Twenty-four hours after MCAO, the mice had developed infarcts affecting the cortex and striatum (Fig. 1A). When administered at 5 min or 3 h after MCAO, BIX significantly reduced the infarct area, infarct volume, and brain swelling, but had no such effect when administered at 6 h (Fig. 1B and D). Our previous results indicate that the induction of BiP by BIX was transient, peaking at 4 h after treatment, but the levels of BiP protein continued to increase until 12 h [9]. Although some drugs for cerebral infarction are permitted for clinical use, most drugs aim to improve the CBF. These drugs must be administered in the early phase of infarction; otherwise they cause adverse effects. For example, t-PA, a most remarkable therapeutic agent for cerebral infarction, must be administered within 3 h after the onset of the infarction, but sometimes causes serious complications such as cerebral hemorrhage [20]. In our previous report, we checked the physiological parameters between control and BIX-treated in permanent MCAO model, and there were no significant differences [9]. It would appear that BIX could save neurons from cell death even if it was given as late as 3 h after the onset of ischemia.

At 24 h after MCAO, an ischemic zone was consistency identified in the cortex (penumbra area) and subcortex (core area) of the left cerebral hemisphere. By measuring infarction, we noted that BIX significantly reduced both the infarct area and the volume in a dose-dependent manner (Fig. 2A and B). Moreover, BIX (intracerebroventricular injection at 20 μg) improved neurological deficits (Fig. 2C). When BIX was administered at 5 min after MCAO, it exhibited dose-dependent neuroprotective effects and, with a dose of 20 μg, reduced both the infarct volume and the neurological deficits significantly. BIX induced BiP mRNA in a concentration-dependent manner; its effects were significant at 1–50 μM [9]. Furthermore, BIX does not induce other ER stress-associated signals (such as XBP-1 splicing or CHOP), and does not evoke ER stress. In cultured human neuroblastoma SK-N-SH cells, BIX at 5 μM inhibited tunicamycin (Tm)-induced cell death [9]. Even a high dosage of BIX at 50 μM did not induce BiP mRNA mediated by non-activating transcription factor 6 pathways [9]. These results imply that the mechanism of BiP induction utilized by BIX may be different from those used by ER stressors, such as thapsigargin and Tm. It has been reported that the activation of transducers of ER stress is caused by dissociation of BiP from luminal domains of PKR (protein kinase regulated by RNA)-like ER-associated kinase and inositol-requiring kinase 1 [2]. It may be assumed that the artificial induction of BiP induced by BIX disturbs the activation of transducers of ER stress, because abundant BiP remains bound to these transducers preventing their activation.

The morphological features of TUNEL-stained cells (indicative of the ischemic damage and apoptotic cell death induced by 24 h MCAO) are shown in Fig. 3B. Cells exhibiting shrunken cell bodies and condensed nuclei were distributed in both the ischemic core and penumbra of the territory affected by MCAO, with the TUNEL-positive cells being among the population displaying such features. Lei et al. [12] reported that numerous cells in the penumbra were TUNEL-positive at 24 h after MCA occlusion, while only a small number of cells in the core were TUNEL-positive at that time. In this study, TUNEL-positive cells (necrotic and apoptotic cells) were

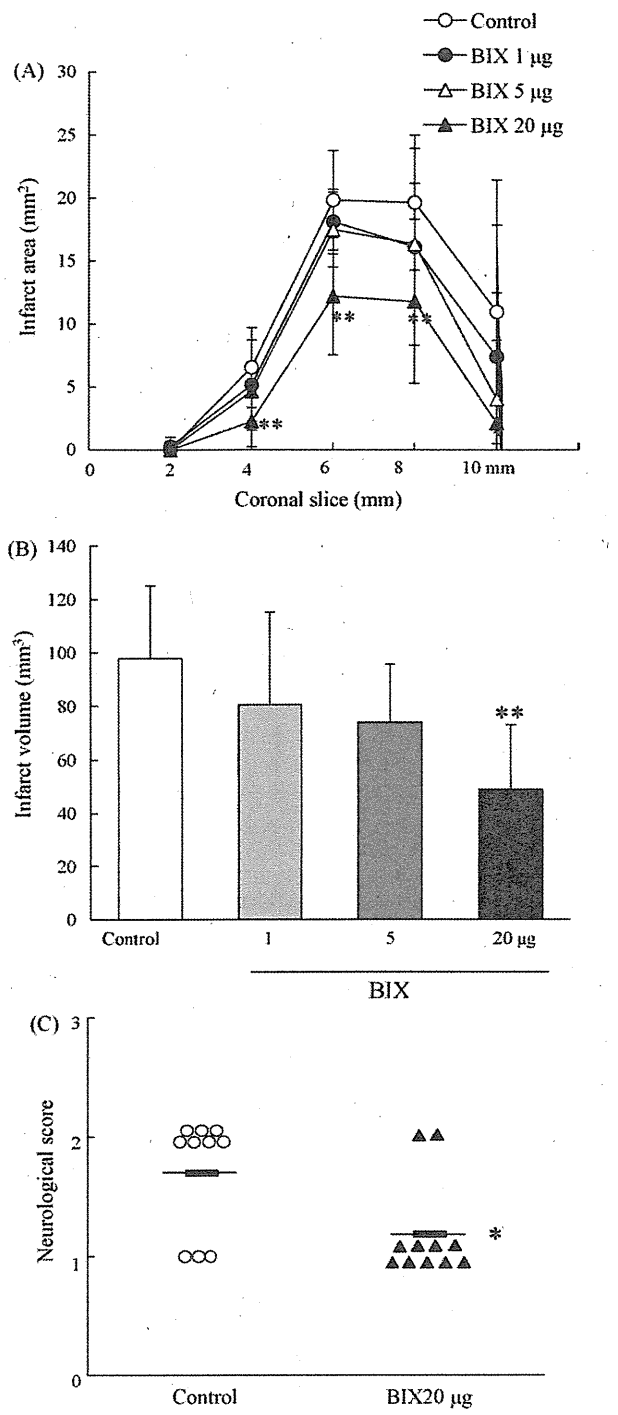

Fig. 2. Effects of BIX administered at 5 min after ischemia on infarction and neuronal damage at 24 h after MCAO in mice. (A) Brain infarct area measured at 24 h after MCA occlusion. Brains were removed and the forebrains sliced into five coronal 2 mm sections. *$P < 0.05$, vs. control (n = 7–11). (B) Effects of BIX on infarct volume (measured at 24 h after MCAO). BIX protected against the decrease in a dose-dependent manner. Values are expressed as the mean ± S.E. **$P < 0.01$ vs. control (n = 7–11). (C) Effects of BIX on neurological score (assessed at 24 h after MCAO). Values are expressed as the mean ± S.D. *$P < 0.05$ vs. control (n = 10–11).

predominantly located in the ischemic core region rather than in the ischemic penumbra, and BIX significantly reduced the number of TUNEL-positive cells in the ischemic penumbra (Fig. 3C). We next distinguished apoptotic cells from necrotic cells, and each type was counted. Only densely labeled cells showing cell shrinkage, chromatin condensation, and fragmented nuclei indicating apoptosis were considered to be apoptotic cells, whereas cells with light dif-

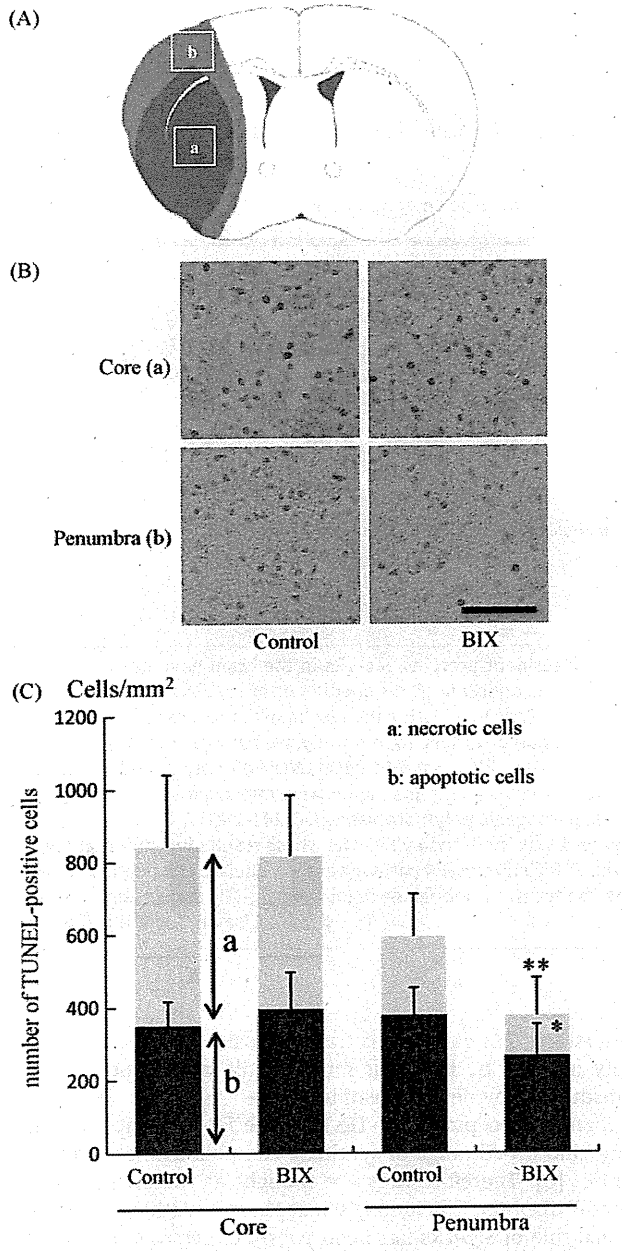

Fig. 3. Effects of BIX on TUNEL staining at 24 h after MCAO in mice. (A) Schematic drawing showing brain regions at 0.4–1.0 mm anterior to bregma (through the anterior commissure): measurement areas (a and b) in Fig. 1A. (B) Representative photomicrographs of TUNEL-positive cells in ischemic core and penumbra. Scale bar = 50 μm. (C) Quantitative analysis of TUNEL-positive cells (necrotic and apoptotic cells). TUNEL-positive cells were significantly reduced in ischemic penumbra at 24 h after MCAO. (a and b): the number of necrotic cells and apoptotic cells, respectively, among all positive cells. Values are expressed as the mean ± S.D. $^{*}P < 0.05$, $^{**}P < 0.01$ vs. control ($n = 7$).

fuse labeling were taken as necrotic. BIX reduced the number of necrotic and apoptotic cells significantly in the ischemic penumbra area at 24 h after MCAO (Fig. 3C).

In conclusion, we suggest that post-treatment of BIX, even if it was administered at 3 h after ischemia, provides significant protection against focal ischemia and has a wide therapeutic window. Hence, drugs which selectively induce BiP may exert a neuroprotective effect and may be the seeds of new treatment of stroke.

References

[1] M.M. Bednar, C.E. Gross, Antiplatelet therapy in acute cerebral ischemia, Stroke 30 (1999) 887–893.
[2] A. Bertolotti, Y. Zhang, L.M. Hendershot, H.P. Harding, D. Ron, Dynamic interaction of BiP and ER stress transducers in the unfolded-protein, Nat. Cell Biol. 2 (2000) 326–332.
[3] M.L. Dyken, Antiplatelet agents and stroke prevention, Semin. Neurol. 18 (1998) 441–450.
[4] C.J. Gomer, A. Ferrario, N. Rucker, S. Wong, A.S. Lee, Glucose regulated protein induction and cellular resistance to oxidative stress mediated by porphyrin photosensitization, Cancer Res. 51 (1991) 6574–6579.
[5] H. Hara, R.M. Friedlander, V. Gagliardini, C. Ayata, K. Fink, Z. Huang, M. Shimizu-Sasamata, J. Yuan, M.A. Moskowitz, Inhibition of interleukin 1beta converting enzyme family proteases reduces ischemic and excitotoxic neuronal damage, Proc. Natl. Acad. Sci. U.S.A. 94 (1997) 2007–2012.
[6] H. Hara, P.L. Huang, N. Panahian, M.C. Fishman, M.A. Moskowitz, Reduced brain edema and infarction volume in mice lacking the neuronal isoform of nitric oxide synthase after transient MCA occlusion, J. Cereb. Blood Flow Metab. 16 (1996) 605–611.
[7] D. Ito, K. Tanaka, S. Suzuki, T. Dembo, A. Kosakai, Y. Fukuuchi, Up-regulation of the Ire1-mediated signaling molecule, Bip, in ischemic rat brain, Neuroreport 12 (2001) 4023–4028.
[8] T Katayama, K. Imaizumi, N. Sato, K. Miyoshi, T. Kudo, J. Hitomi, T. Morihara, T. Yoneda, F. Gomi, Y. Mori, Y. Nakano, J. Takeda, T. Tsuda, Y. Itoyama, O. Murayama, A. Takashima, P. St George-Hyslop, M. Takeda, M. Tohyama, Presenilin-1 mutations downregulate the signalling pathway of the unfolded-protein response, Nat. Cell Biol. 1 (1999) 479–485.
[9] T. Kudo, S. Kanemoto, H. Hara, N. Morimoto, T. Morihara, R. Kimura, T. Tabira, K. Imaizumi, M. Takeda, A molecular chaperone inducer protects neurons from ER stress, Cell Death Differ. 15 (2008) 364–375.
[10] A.S. Lee, The glucose-regulated proteins: stress induction and clinical applications, Trends Biochem. Sci. 26 (2001) 504–510.
[11] A.S. Lee, Mammalian stress response: induction of the glucose-regulated protein family, Curr. Opin. Cell Biol. 4 (1992) 267–273.
[12] B. Lei, S. Popp, C. Capuano-Waters, J.E. Cottrell, I.S. Kass, Lidocaine attenuates apoptosis in the ischemic penumbra and reduces infarct size after transient focal cerebral ischemia in rats, Neuroscience 125 (2004) 691–701.
[13] L.J. Li, X. Li, A. Ferrario, N. Rucker, E.S. Liu, S. Wong, C.J. Gomer, A.S. Lee, Establishment of a Chinese hamster ovary cell line that expresses grp78 antisense transcripts and suppresses A23187 induction of both GRP78 and GRP94, J. Cell. Physiol. 153 (1992) 575–582.
[14] R.V. Rao, A. Peel, A. Logvinova, G. del Rio, E. Hermel, T. Yokota, P.C. Goldsmith, L.M. Ellerby, H.M. Ellerby, D.E. Bredesen, Coupling endoplasmic reticulum stress to the cell death program: role of the ER chaperone GRP78, FEBS Lett. 514 (2002) 122–128.
[15] R.K. Reddy, C. Mao, P. Baumeister, R.C. Austin, R.J. Kaufman, A.S. Lee, Endoplasmic reticulum chaperone protein GRP78 protects cells from apoptosis induced by topoisomerase inhibitors: role of ATP binding site in suppression of caspase-7 activation, J. Biol. Chem. 278 (2003) 20915–20924.
[16] M. Shibata, H. Hattori, T. Sasaki, J. Gotoh, J. Hamada, Y. Fukuuchi, Activation of caspase-12 by endoplasmic reticulum stress induced by transient middle cerebral artery occlusion in mice, Neuroscience 118 (2003) 491–499.
[17] T. Steiner, E. Bluhmki, M. Kaste, D. Toni, P. Trouillas, R. von Kummer, W. Hacke, The ECASS 3-hour cohort. Secondary analysis of ECASS data by time stratification. ECASS Study Group. European Cooperative Acute Stroke Study, Cerebrovasc. Dis. 8 (1998) 198–203.
[18] S. Sugawara, K. Takeda, A. Lee, G. Dennert, Suppression of stress protein GRP78 induction in tumor B/C10ME eliminates resistance to cell mediated cytotoxicity, Cancer Res. 53 (1993) 6001–6005.
[19] S. Tajiri, S. Oyadomari, S. Yano, M. Morioka, T. Gotoh, J.I. Hamada, Y. Ushio, M. Mori, Ischemia-induced neuronal cell death is mediated by the endoplasmic reticulum stress pathway involving CHOP, Cell Death Differ. 11 (2004) 403–415.
[20] N. Wahlgren, N. Ahmed, A. Davalos, G.A. Ford, M. Grond, W. Hacke, M.G. Hennerici, M. Kaste, S. Kuelkens, V. Larrue, K.R. Lees, R.O. Roine, L. Soinne, D. Toni, G. Vanhooren, Thrombolysis with alteplase for acute ischaemic stroke in the Safe Implementation of Thrombolysis in Stroke-Monitoring Study (SITS-MOST): an observational study, Lancet 369 (2007) 275–282.
[21] Z. Yu, H. Luo, W. Fu, M.P. Mattson, The endoplasmic reticulum stress-responsive protein GRP78 protects neurons against excitotoxicity and apoptosis: suppression of oxidative stress and stabilization of calcium homeostasis, Exp. Neurol. 155 (1999) 302–314.

Biochemical and Biophysical Research Communications 415 (2011) 519–525

Contents lists available at SciVerse ScienceDirect

Biochemical and Biophysical Research Communications

journal homepage: www.elsevier.com/locate/ybbrc

Sigma-1Rs are upregulated via PERK/eIF2α/ATF4 pathway and execute protective function in ER stress

Teruhiko Mitsuda *, Tsubasa Omi, Hitoshi Tanimukai, Yukako Sakagami, Shinji Tagami, Masayasu Okochi, Takashi Kudo, Masatoshi Takeda

Psychiatry, Department of Integrated Medicine, Division of Internal Medicine, Osaka University Graduate School of Medicine, Osaka 565-0871, Japan

ARTICLE INFO

Article history:
Received 21 October 2011
Available online 3 November 2011

Keywords:
Sigma-1 receptor
Transcription factor
ATF4
Mental disorders
ER stress
Protective function

ABSTRACT

Sigma-1 receptors (Sig-1Rs) are the ER resident proteins. Sig-1Rs in the brain have been reported to be significantly reduced in patients with schizophrenia. The impediment of regulating Sig-1Rs expression levels increases the risk for schizophrenia. Thus elucidating the mechanism regulating Sig-1Rs expression might provide the strategy to prevent mental disorders. In this study, we have demonstrated that Sig-1Rs were transcriptionally upregulated by ATF4 in ER stress. Moreover, ATF4 directly bounds to the 5′ flanking region of *Sig-1R* gene. The reporter activities using this region were enhanced in ER stress, or by ATF4 alone. The reporter activities with the pathogenic polymorphisms (GC-241-240TT, T-485A) were reduced. In addition, the processing of Caspase-4 was inhibited by Sig-1Rs. These results indicate that Sig-1Rs are transcriptionally upregulated via the PERK/eIF2α/ATF4 pathway and ameliolate cell death signaling. This study is the first report identifying the transcription factor regulating Sig-1Rs expression.

1. Introduction

The endoplasmic reticulum (ER) is a cellular compartment involved in the localization and folding of proteins [1,2]. Cellular stress conditions lead to the accumulation of unfolded proteins in the ER, thereby representing a fundamental threat to cell viability. To avoid the excessive accumulation of unfolded proteins in the ER, eukaryotic cells have signaling pathways. This process is referred to as the unfolded protein response (UPR) [3,4]. The UPR consists of the following three pathways: (1) suppression to generate more proteins; (2) the induction of protective proteins to refold proteins; and (3) activation of the degradation of unfolded proteins by ubiquitin–proteasome pathway. If these strategies fail, cells go into ER stress-induced apoptosis.

Dysfunction of UPR is considered as one of the candidate cascades related to the pathology of mental disorders [5]. The patients with Wolfram syndrome (WS), who have mutations for wolframin gene, encoding ER chaperone, have severe psychiatric symptoms [5].

Reduced induction of XBP-1, the transcription factor which induce ER chaperone, is involved in pathophysiology of bipolar disorder [6] and depression [7]. The reason that dysfunction of UPR increases the risk of mental disorders has not been clearly understood, but continuous translational attenuation and cell fragility induced by ER stress might result in dysfunction of signal transduction by neurotransmitters.

Sigma-1 receptors (Sig-1Rs) are the ER resident proteins. And they bind broad range of synthetic compounds including antipsychotics [8]. Therefore they are thought as therapeutic target for mental disorders, including schizophrenia. Although the physiological role of Sig-1Rs has been poorly understood, recent studies support that Sig-1Rs play pivotal roles in neuroprotection [9,10].

In postmortem studies, Sig-1Rs in the brain have been reported to be reduced in patients with schizophrenia [11]. In genetic association studies, two functional polymorphisms on the 5′ flanking region of the transcription start site of *Sig-1R* gene were detected: GC-241-240TT and T-485A, were found to be associated with schizophrenia [12,13]. Thus the impediment of Sig-1Rs expression are thought as one of pathogenesis for schizophrenia.

In this study, we tried to elucidate the mechanism to regulate Sig-1Rs expression, and verified its protective role.

2. Materials and methods

2.1. Cell culture and chemicals

HEK293 cells or mouse neuroblastoma (Neuro2a) cells were cultured in DMEM (Invitrogen) with 10% FCS at a density of 1×10^6 cells/well in 6-well plates. We used tunicamycin (Tm) (1 μg/ml) or thapsigargin (Tg) (1 μM) (SIGMA) as ER stressors.

* Corresponding author. Fax: +81 6 6879 3051.
E-mail addresses: te_mitsu@yahoo.co.jp, tmitsuda@psy.med.osaka-u.ac.jp (T. Mitsuda).

0006-291X/$ - see front matter © 2011 Elsevier Inc. All rights reserved.
doi:10.1016/j.bbrc.2011.10.113

2.2. Immunoblotting

For Immunoblotting, cells were lysed with RIPA buffer (Thermo scientific) with the protease inhibitor and the phosphatase inhibitor (Roche). The lysates were incubated on ice for 15 min. After centrifugation at 13,000*g* for 20 min, the soluble proteins were loaded onto SDS–polyacrylamide gels. Antibodies against the following proteins were used: Sig-1R from Abcam (1:250), PERK (1:1000; Cell Signaling), phospho-PERK (1:1000; Santa Cruz) eIF2α (1:1000; Cell Signaling), phospho-eIF2α (1:1000; Cell Signaling), ATF4 (1:1000; SantaCruz), CHOP (1:1000; SantaCruz) GAPDH (1:2500 Thermo scientific). Specific antigen-antibody complexes were visualized using HRP-conjugated secondary antibodies and ECL plus kit (GE Healthcare).

2.3. RNA extraction and semi-quatitative RT-PCR

Total RNA was extracted from cells by TRIzol reagent (Invitrogen), according to the manufacturer's protocol. For each extraction, RNA concentration was determined spectrophotometrically at 260 nm, and 2 μg of RNA was used for reverse transcription reaction with PrimeScript II 1st strand cDNA Synthesis Kit (Takara). PCR was performed in a total volume of 50 μl with Ex-Taq polymerase (Takara) using each specific primer set as described in supplemental Table S1.

The PCR was performed for 25 cycles of 30 s at 95 °C, 30 s at 57 °C, and 1 min at 72 °C.

2.4. Transfection

Transfection was performed using calcium phosphate reagent (Invitrogen).

2.5. Knock down of ATF4

ATF4-shRNA-pSuper (Oligoengene) plasmids were transfected into cells to generate ATF4 knockdown cells as previously described [14]. Oligonucleotide used are described in supplemental Table S1.

2.6. Chromatin immunoprecipitation assay

Assay was performed using Chip-IT kit (active motif) according to manufacturer's instruction. Briefly, cells transfected with ATF4 expression plasmids were fixed in 1% formaldehyde/HBSS and then homogenized and sheared with sonication. Chromatin was precipitated with anti-ATF4 antibody (1:200), or rabbit IgG (Santa Cruz Biotechnology). The human *Sig-1R* promoter region from bp −582 to −156 (the number is the distance in base pairs from the putative transcription start site, +1) was amplified by PCR with primers as described in supplemental Table S1.

2.7. Luciferase assay

5′ Upstream region of human *Sig-1R* gene (from −582 to −156) was subcloned into upstream of firefly luciferase in pGL4.12 vector. The reporter plasmids were transfected into HEK293 cells. pRL-TK were co-transfected to correct transfection efficiency.

Forty-eight hours after transfection, luciferase assay was performed using the Dual-Luciferase Reporter Assay System (Promega) and Wallac 1420 ARVOsx luminometer (Perkin–Elmer).

2.8. Statistical analysis

To determine whether the treatment was significantly different from the control, 2-tailed paired Student's *t* test was used. A *P* value less than 0.05 was considered statistically significant. In the figures, the intensity of bands was quantified by Adobe Photoshop software. All graphical data are shown as mean ± S.D.

3. Results

3.1. Sig-1Rs expression increases in ER stress

We first performed a time course analysis of Sig-1Rs expression levels during ER stress. HEK 293 cells were treated with tunicamycin (Tm, N-glycosylation inhibitor) to induce ER stress, for 15, 30, 60, and 120 min. Lysates were subjected to immunoblot analysis. In order to monitor the induction of ER stress, we observed activation of PERK-eIF2α pathway and induction of ATF4 and BiP (Grp78 and Grp94). In the early stage in ER stress, PERK, the ER resident kinase is phosphorylated, then transduce the signaling to eIF2α. Phosphorylated eIF2α selectively activates ATF4 translation [15].

After treatment with Tm, Sig-1Rs expression was immediately and dramatically induced (Fig. 1A and B). This upregulation was observed within 30 min, and peaked after 60 min. And phosphorylation of PERK and phosphorylation of eIF2α was observed within 30 min. In addition to these results, translation of ATF4 was also activated within 60 min. These data indicated that ER stress was sufficiently induced after 60 min with Tm. In this condition, Sig-1Rs expression was simultaneously induced. BiP is an ER chaperon that does not express under normal conditions; however, we detected BiP expression, this result also supported that ER stress was actually induced.

3.2. Induction of Sig-1Rs is also verified in neuronal cells

Sig-1Rs are widely expressed in central nervous system, including hypocampus and frontal cortex [16]. And dysregulation of Sig-1Rs expression are thought as one of pathogenesis for mental disorders. Next, in order to verify the replicative of Sigma-1Rs induction in neuronal cells, we used neuroblastoma Neuro2a cells. Neuro2a cells were treated with another ER stressor, thapsigargin (Tg), an inhibitor of ER Ca^{2+}-ATPase. Similarly in HEK 293 cells treated with Tm, phosphorylation of PERK and eIF2α, translation of ATF4 was immediately observed after treatment with Tg within 60 min (Fig. 1C). Interestingly, Sigma-1Rs expression was induced within 60 min (Fig. 1C and D). Induction of Sig-1Rs was also observed in neuronal cells regardless of the ER stressor types.

3.3. Sig-1R is transcriptionally upregulated

In genetic association studies, polymorphic sites located on the 5′ flanking region of the transcription start site in *Sig-1R* gene have been detected. Therefore, we hypothesized that upregulation of Sig-1Rs expression in ER stress was due to transcriptional activation. We performed semi-quantitative RT-PCR to measure *Sigma-1R* mRNA levels. To monitor the induction of ER stress, we monitored the splicing of *Xbp1 mRNA*.

Xbp1 is a transcription factor; it is activated by spliceosome-independent mRNA splicing initiated by Ire1α in ER stress [17]. Xbp1 protein from the spliced mRNA (Xbp1s protein) is a potent transcription factor inducing expression of UPR-related genes. After treatment with Tm, the mRNA levels spliced *Xbp-1* were gradually up-regulated (Fig. 1E). This result indicated that ER stress actually occurred in this condition.

Sig-1R mRNA levels were immediately and dramatically upregulated within 30 min, and peaked at 60 min (Fig. 1E and F).

Our data regarding upregulation of mRNA levels of *Sig-1R* indicated that transcription of *Sig-1R* gene was induced immediately in the acute phase of ER stress.

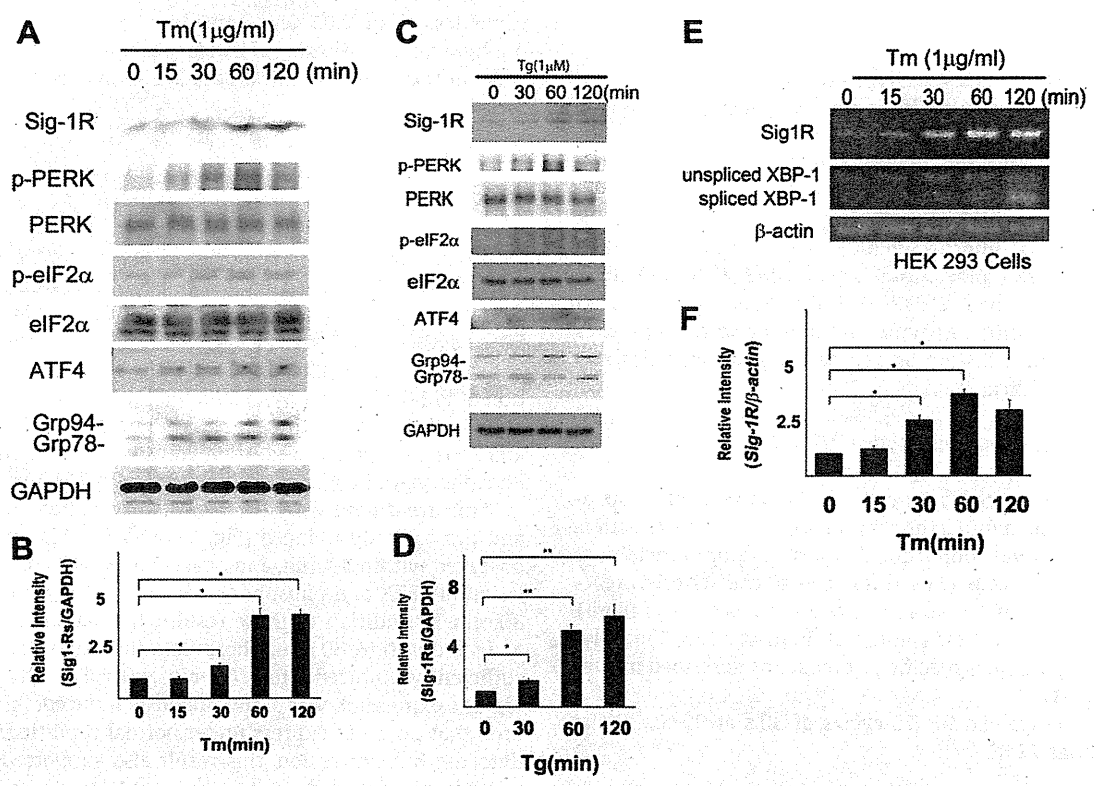

Fig. 1. Sig-1Rs increases in ER stress. (A) Time course of Sig-1Rs upregulation in HEK293 cells with Tm treatment. Cells were treated with 1 μg/ml Tm, for the indicated period. Sig-1Rs protein levels were elevated in ER stress. (B) Sig-1Rs protein levels in Fig. 1A were quantified; values are means ± S.D. (*$p < 0.05$, **$p < 0.01$, $n = 3$). (C) Time course of Sig-1Rs upregulation in Neuro2a cells with Tg treatment. Cells were treated with 1 μM Tg, for the indicated period. Sig-1Rs protein levels were elevated in ER stress. (D) Sig-1Rs protein levels in Fig. 1C were quantified; values are means ± S.D. (*$p < 0.05$, **$p < 0.01$, $n = 3$). (E) Time course of Sig-1R mRNA induction in HEK293 cells with Tm treatment is shown by semi-quantitative RT-PCR. Cells were treated with 1 μg/ml Tm, for the indicated period. Sig-1R mRNA levels were elevated in ER stress. (F) Sig-1R mRNA levels in Fig. 1E were quantified; values are means ± S.D. (*$p < 0.05$, **$p < 0.01$, $n = 3$).

3.4. ATF4 is the pivotal transcription factor for Sig-1R gene expression in ER stress

In order to understand the molecular mechanism underlying this transcriptional regulation, we next tried to identify the transcription factor that activates *Sig-1R* transcription. In ER stress, ATF4, ATF6, and XBP-1 are known as major transcription factors which induce expression of UPR-related genes [18–20]. HEK293 cells were transfected with the expression plasmids for ATF4, ATF6, and XBP-1, then subjected to immunoblot analysis.

Forty-eight hours after transfection, we confirmed that Sigma-1Rs expression was increased in accordance with ATF4 expression (Fig. 2B). Only ATF4 induced Sig-1Rs expression. ATF6 and XBP-1 did not induce Sigma-1Rs expression (data not shown).

Under ER stress, three UPR pathways are known, PERK-eIF2α-ATF4 pathway, Ire1α pathway, and ATF6 pathway. Among these pathways, PERK-eIF2α-ATF4 pathway is promptly activated in the acute phase of ER stress.

From our data regarding expression of Sig-1Rs in ER stress, Sig-1Rs were immediately induced in the acute phase of ER stress. And among transcription factors which work in ER stress, only ATF4 induced expression of Sig-1Rs. These results were consistent with the fact that PERK-eIF2α-ATF4 pathway is preferentially activated in the acute phase of ER stress.

3.5. Knock down of ATF4 results in decreased Sig-1R level

In order to confirm upregulation of Sigma-1Rs is controlled by ATF4, we generated ATF4 knock down HEK 293 (ATF4KD) cells. The shRNA expression plasmids for ATF4 or control shRNA were transfected into cells. We compared the expression levels of Sig-1Rs in ATF4KD cells with control cells by immunoblotting. In control cells, induction of ATF4 was observed after Tm treatment, simultaneously phosphorylation of PERK and eIF2α were observed (Fig. 2C). But in ATF4 knock down (ATF4KD) cells, induction of ATF4 was not observed after Tm treatment, nevertheless phosphorylation of PERK and eIF2α were observed (fig. 2C). In this condition, the expression levels of Sig-1Rs in control cells were upregulated after Tm treatment. But in ATF4KD cells, the upregulation of Sigma-1Rs was cancelled nevertheless ER stress was actually induced (Fig. 2C and D). These results indicated that ATF4 was necessary for the induction of Sig-1Rs in ER stress.

3.6. ATF4 directly binds to 5′ upstream region of Sig-1R

In genetic association studies, two polymorphic sites in the 5′ flanking region of *Sig-1R* gene were found to be associated with schizophrenia. We hypothesized that the recruitment of ATF4 to the 5′ flanking region of *Sig-1R* gene is critical for transcriptional activation. We tried to confirm whether ATF4 directly binds to the region including these polymorphic sites (−582 to −156) of *Sigma-1R* gene (Fig. 2A). The chromatin immunoprecipitaion assay was performed. The 5′ flanking region of *Sig-1R* gene (−582 to −156) was amplified by PCR with immunoprecipitated chromatin-transcription factor complex. As shown in Fig. 2E, a 426-bp DNA fragment corresponding to the 5′ upstream region of *Sig-1R* gene (−582 to −156) was detected in immunoprecipitated complex with anti-ATF4 antibody. But no bands were observed in the complex with IgG, used as negative control (Fig. 2E). This result indicated that ATF4 directly bound to the 5′ upstream region of *Sig-1R* gene.

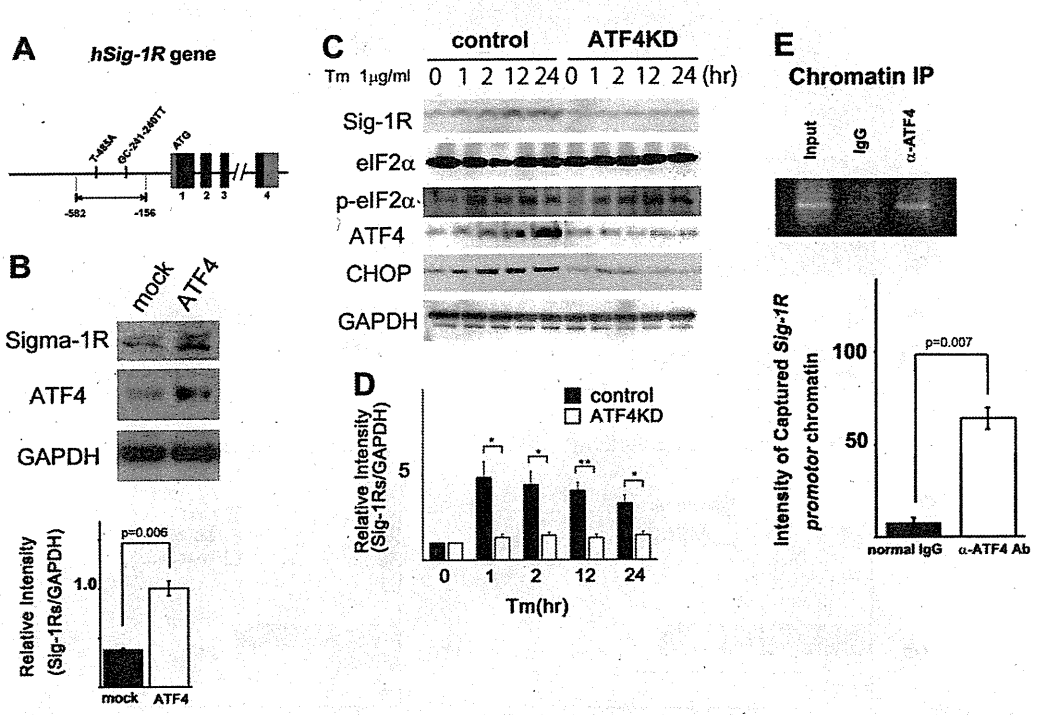

Fig. 2. ATF4 is the pivotal transcription factor for Sig-1Rs expression. (A) Schematic representation of human Sig-1R gene. Two functional polymorphisms of the Sig-1R genotype are known; GC-241-240TT and T-485A, were found to be associated with schizophrenia. (B) Upregulation of Sig-1Rs in HEK293 cells transfected with ATF4. Cells were transfected with plasmids encoding full-length ATF4 or mock. Forty-eight hours after transfection, overexpression of ATF4 results in the increase of expression levels of Sig-1Rs protein; values are means ± S.D. ($n = 3$). (C) Cancellation of Sig-1Rs upregulation in ATF4KD cells. Sig-1Rs upregulation could not be observed in ATF4KD cells nevertheless with Tm treatment. (D) Sig-1Rs protein levels in Fig. 2C were quantified; values are means ± S.D. ($^*p < 0.05$, $^{**}p < 0.01$, $n = 3$). (E) ChIP assay was performed with anti-ATF4 antibody. Positive band was observed in precipitates with anti-ATF4 antibody, but not with control IgG; values are means ± S.D. ($n = 3$).

3.7. The promoter region of Sig-1R (-582 to-156) is sufficient for induction of Sig-1R gene

From these results, we next tried to determine that the promoter region of *Sig-1R* gene (−582 to −156) is sufficient to activate transcription of *Sig-1R* by reporter assay.

The promoter region was fused with the firefly luciferase plasmid (Fig. 3A). This reporter plasmid was introduced into HEK293 cells, and then treated with tunicamycin for 2 h to induce ER stress. Relative luciferase activity was enhanced to 7.2 fold, compared with cells treated with DMSO (Fig. 3A). We next determined that this region is sufficient to activate transcriptional activity of *Sig-1R* by ATF4. The expression plasmids for ATF4 was co-transfected with this reporter plasmids intoHEK293 cells. Relative luciferase activity was enhanced to 8.8 fold, compared with cells co-transfected with mock plasmids (Fig. 4A).

3.8. Knock down of ATF4 results in decreased reporter activity

In order to verify that ATF4 is essential for transcriptional activation of *Sig-1R* gene by interaction with this promoter region, we measured the reporter activity in ATF4 knock down cells. The shRNA expression plasmids for ATF4 or control shRNA were co-transfected with the reporter plasmid into cells. Forty-eight hours after transfection, cells were treated with Tm for 2 h. We compared the relative luciferase activity in ATF4KD cells with control cells (Fig. 3B). In the control cells, the luciferase activity was enhanced. This result was consistent with our data with Immunoblotting. Whereas the upregulation of luciferase activity was not observed in the ATF4KD cells (Fig. 3B). The inhibition of ATF4 expression resulted in the cancellation of the enhancement of reporter activity. This result supported that ATF4 was essential for transcriptional activation of *Sig-1R* gene.

3.9. Induction of reporter activity in ER stress was decreased in pathogenic polymorphisms

As mentioned above, two polymorphisms in *Sig-1R* gene, GC-241-240TT and T-485A are thought to be associated with schizophrenia. These polymorphisms are located on the 5′ upstream region of the transcription start site.

To determine the effect of these polymorphisms on the transcription of the human *Sig-1R* in ER stress, the plasmids corresponding to two haplotypes (T-485A, GC-241-240TT) were generated by the mutagenesis (Fig. 3C), and transfected into HEK 293 cells to measure reporter activity. Forty-eight hours after transfection, cells were treated with Tm for 2 h. We compared the relative luciferase activity in the cells transfected with the plasmids corresponding to two haplotypes (T-485A, GC-241-240TT) to wild type cells (Fig. 3C).

In WT cells, luciferase activity was enhanced to 7.2 fold, but in the cells corresponding to two haplotypes, enhancement of activity was decreased (4.2 fold in T-485A, and 2.7 fold in GC-241-240TT).

3.10. Induction of reporter activity by ATF4 was decreased in pathogenic polymorphisms

In Fig. 2, we verified that ATF4 directly bound to the 5′ flanking region (−582 to −156) and induced Sig-1Rs expression. We next tried to determine the effect of pathogenic polymorphisms (T-485A, GC-241-240TT) on the binding with ATF4 and transcriptional activation. The each reporter plasmids (WT, T-485A, or GC-241-240TT) were co-transfected with ATF4 expression plasmids. Forty-eight hours after transfection, we compared luciferase activity.

In WT cells, luciferase activity was enhanced to 9.1 fold, but in the cells corresponding to pathogenic haplotypes, enhancement of activity was decreased as shown in Fig. 3D (3.4 fold in T-485A, and

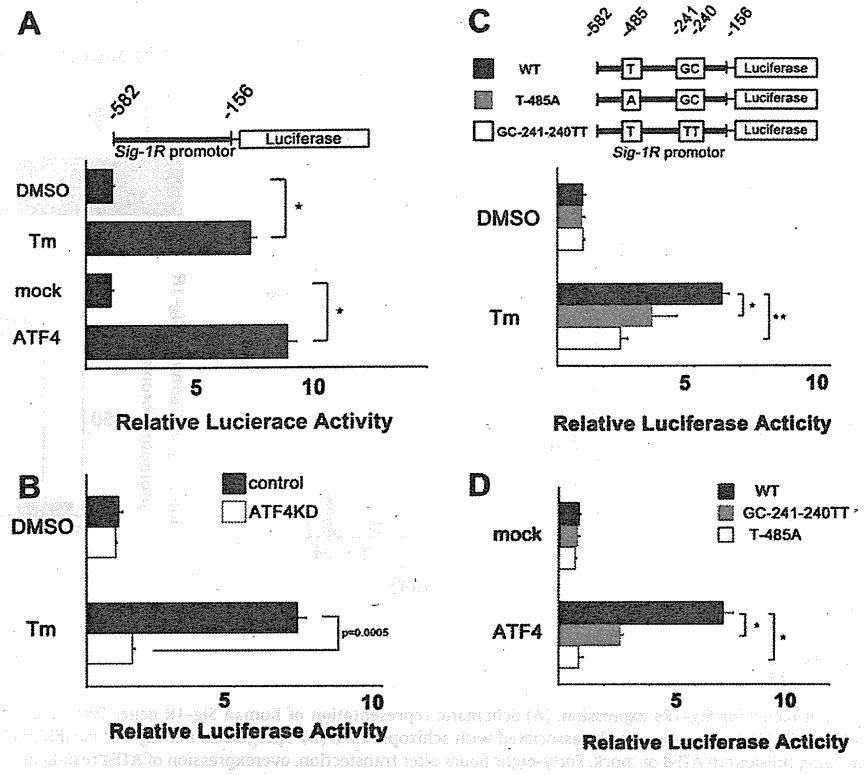

Fig. 3. (A) The promoter region of Sig-1R (−582 to −156) is sufficient for induction of Sig-1R gene. The promoter region was fused with the firefly luciferase plasmid. Luciferase activity was enhanced to 7.2 fold with Tm treatment. And with ATF4 transfection, luciferase activity was enhanced to 8.8 fold. (*$p < 0.01$, $n = 3$) (B) Knock down of ATF4 results in decreased activity. Luciferase activity in ATF4KD cells and control cells were compared. The inhibition of ATF4 expression resulted in the cancellation of the enhancement of reporter activity. (C) Induction of reporter activity in ER stress was decreased in pathogenic polymorphisms. Cells were treated with Tm for 2 h. We compared luciferase activity in the cells transfected with the plasmids corresponding to two haplotypes (T-485A, GC-241-240TT) to wild type cells. In WT cells, relative luciferase activity was enhanced to 7.2 fold, but in the cells corresponding to two haplotypes, enhancement of activity was decreased (4.2 fold in T-485A, and 2.7 fold in GC-241-240TT). (*$p < 0.05$, **$p < 0.01$, $n = 3$) (D) Induction of reporter activity by ATF4 was decreased in pathogenic polymorphisms. The each reporter plasmids (WT, T- 485A, or GC-241-240TT) were co-transfected with ATF4 expression plasmids. In WT cells, relative luciferase activity was enhanced to 9.1 fold, but in the cells corresponding to pathogenic haplotypes, enhancement of activity was decreased (3.4 fold in T-485A, and 0.9 fold in GC-241-240TT). (*$p < 0.01$, $n = 3$).

0.9 fold in GC-241-240TT). In pathogenic allele (-485A, -421-240TT), transcriptional activation of of *Sig-1R* gene was decreased. These results indicated that these polymorphic sites (-485T, -241-240GC) were pivotal for transcriptional activation of *Sig-1R* gene by ATF4.

3.11. Sig-1Rs inhibits Caspase-4 processing

Finally, we tried to elucidate the physiological role of Sig-1Rs in ER stress. Caspases are a family of proteins that are the main executors of the apoptotic process. Caspase-4 is thought as ER stress-specific Caspase [21].

So we compared processing of Caspase-4 in ER stress between Sigma-1Rs transfectant and mock transfectant. We generated HEK 293 cells stably expressing Sig-1Rs.

As shown in Fig. 4A, Caspase-4 was processed after Tm treatment in mock control, but in Sigma-1Rs transfectant, processed Caspase-4 was prominently decreased (Fig. 4A and B).

This result indicates that induction of Sig-1Rs inhibited Caspase-4 processing to ameliolate cell death signaling.

4. Discussion

Result of the present study has provided the clue to exploit the mechanism to regulate Sig-1Rs expression and the role of Sig-1Rs. The expression of Sig-1Rs was induced via PERK-eIF2α-ATF4 pathway in ER stress, to execute protective function (Fig. 4C).

In this study, induction of Sig-1Rs in ER stress was observed within 60 min. This results regarding time course analysis of Sig-1Rs induction were unexpected for us. Sig-1Rs were more rapidly upregulated than our expectation. Sig-1Rs might be immediately induced in acute phase of ER stress to collect cellular dysfunction. The reason that dysfunction of UPR increases the risk of mental disorders has not been clearly understood, but continuous translational attenuation and cell fragility induced in ER stress might result in dysfunction of signal transduction by neurotransmitters. And the reason that the decrease of Sig-1Rs expression levels increases the risk of mental disorders has also not been clearly understood. Sig-1Rs are immediately upregulated in acute phase ER stress, and collect cellular dysfunction due to continuous translational attenuation and cell fragility.

We focused about upregulation of Sig-1Rs by ATF4 in ER stress. But eIF2α-ATF4 is activated not only in ER stress. There are three known eIF2α kinases other than PERK: protein kinase R(PKR), heme-regulated eIF2α kinase(HRI), and GCN2(general control nonderepressible-2) [22,23], all of which are activated by distinct forms of stress. Upregulation of Sig-1Rs by ATF4 might be also activated via these pathways, and Sig-1Rs might play protective role in various stress; not only ER stress.

In previous studies, not only Sig-1Rs, ATF4 was reported to be associated with schizophrenia [24]. One possible explanation is that Sig-1Rs induction by ATF4 might be disturbed in the patient with pathogenic allele. Dysregulation of this protective pathway (ATF4-Sig-1Rs) might increase the risk of schizophrenia.

In luciferase reporter assay, we identified that 5′ promoter region (−582 to −156) is important to induce *Sig-1R* expression in ER stress by ATF4. In the chimeric mutant corresponding the